Journal Pre-proofs

Leveraging a multivariate approach towards enhanced development of direct compression extended release tablets

A.S. Sousa, J. Serra, C. Estevens, R. Costa, A.J. Ribeiro

PII: S0378-5173(23)00853-0
DOI: https://doi.org/10.1016/j.ijpharm.2023.123432
Reference: IJP 123432

To appear in: *International Journal of Pharmaceutics*

Received Date: 21 June 2023
Revised Date: 16 September 2023
Accepted Date: 19 September 2023

Please cite this article as: A.S. Sousa, J. Serra, C. Estevens, R. Costa, A.J. Ribeiro, Leveraging a multivariate approach towards enhanced development of direct compression extended release tablets, *International Journal of Pharmaceutics* (2023), doi: https://doi.org/10.1016/j.ijpharm.2023.123432

Leveraging a multivariate approach towards enhanced development of direct compression extended release tablets

Sousa, A.S.[1,2], Serra, J.[2], Estevens, C.[2], Costa, R.[2], Ribeiro, A.J.[1,3]*

[1] Universidade de Coimbra, Faculdade de Farmácia, 3000-148 Coimbra, Portugal;

[2] Grupo Tecnimede, Quinta da Cerca, Caixaria, 2565-187 Dois Portos, Portugal;

[3] i3S, IBMC, Rua Alfredo Allen, 4200-135 Porto, Portugal.

* Corresponding author:

António J. Ribeiro

Universidade de Coimbra

Faculdade de Farmácia, Portugal.

E-mail address: aribeiro@ff.uc.pt

Abstract

Extended release formulations play a crucial role in the pharmaceutical industry by maintaining steady plasma levels, reducing side effects, and improving therapeutic efficiency and compliance. One commonly used method to develop extended release formulations is direct compression, which offers several advantages, such as simplicity, time savings, and cost-effectiveness. However, successful direct compression-based extended release formulations require careful assessment and an understanding of the excipients' attributes. The scope of this work is the characterization of the compaction behavior of some matrix-forming agents and diluents for the development of extended release tablets. Fifteen excipients commonly used in extended release formulations were evaluated for physical, compaction and tablet properties. Powder properties (e.g., particle size, flow properties, bulk density) were evaluated and linked to the tablet's mechanical properties in a fully integrated approach, and data were analyzed by constructing a principal component analysis (PCA). Significant variability was observed among the various excipients. The present work successfully demonstrates the applicability of PCA as an effective tool for comparative analysis, pattern and clustering recognition and correlations between excipients and their properties, facilitating the development and manufacturing of direct compressible extended release formulations.

Keywords

Extended release; Excipient characterization; Direct compression; Multivariate data analysis; Principal component analysis

1. Introduction

Excipients, once questioned about their functionality, are now recognized to play a central role in the manufacture, stability and/or *in vitro* and *in vivo* performance of pharmaceutical formulations. The diversity observed in pharmaceutical excipients, along with their physicochemical properties and innate variability can have a significant effect on the quality of the final drug product (Thakkar et al., 2016). It is acknowledged that a given excipient can be used in different ways because its functionality is understood according to specific drug product formulation and manufacturing (Zhao et al., 2022). Recognizing the importance of assessing and controlling excipient functionality, both the European Pharmacopeia (Ph. Eur.) and the United States Pharmacopeia (USP) have adopted the concept of Functionality-Related Characteristics (FRCs). This concept emphasizes the growing awareness of the importance of a systematic, scientific and risk-based Quality by Design (QbD) approach, providing a comprehensive understanding of excipient attributes for improved and controlled drug product quality throughout its lifecycle (Moreton, 2010). A deep knowledge of FRCs, as critical material attributes (CMAs), is crucial not only to support formulation development but also for evaluating the potential effect of excipient variability on drug product quality. Accordingly, excipients should be incorporated as an important part of the QbD design space, and their variability needs to be built into the design space (Carlin, 2018; Kim and Choi, 2022a; Moreton, 2010).

Oral extended release delivery systems have steadily increased in importance over the years. It offers an opportunity to significantly improve patient compliance and therapeutic outcomes. The complexity of oral extended release drug delivery systems development makes the implementation of the QbD framework, including risk assessment, design of experiments (DoE) and multivariate data analysis (MVDA), essential to better understand the product and process parameters (Sousa et al., 2022). Generally, the simplest extended release formulations, excluding the lubricant, consist of a ternary system comprising the active pharmaceutical ingredient (API), matrix former polymer responsible for drug release kinetics, and diluent ensuring rheological properties. The typical percentage of polymer ranges from 20% to 50%, with the remaining percentage comprising the diluent and API, depending on the dosage and manufacturing processing properties (Colombo et al., 2008; Maderuelo et al., 2011; Timmins et al., 2014). Studies have been carried out to explore the effect of raw material properties on extended release matrix tablet performance (Maderuelo et al., 2011; Thakkar et al., 2016; Tobyn et al., 2018; Vanza et al., 2020; Zhang et al., 2018; Zhou et al., 2014). Some of the most relevant FRCs of polymers include molecular weight (MW) (Vanza et al., 2020; Zhou et al., 2014), viscosity (Kosir et al., 2018; Zhou et al., 2014), hydration (Vanza et al., 2020), particle size (Haware et al., 2010; Kosir et al., 2018; Zhang et al., 2018), powder flow (Zhang et al., 2019; Zhang et al., 2018) and degree of substitution of the polymer side chain (Caccavo et al., 2017; Kosir et al., 2018; Zhou et al., 2014). Additionally, excipient variability among different manufacturers, grades, batches and lots can significantly affect the functionality and performance of extended release dosage forms (Dave et al., 2015; Zhou et al., 2014). To support the QbD approach and control raw material variability, several studies are now using MVDA and/or artificial neural network (ANN)

(Benedetti et al., 2019; Haware et al., 2010; Kim and Choi, 2022a, b; Portier et al., 2021; Tobyn et al., 2018; Wan et al., 2021; Wang et al., 2020; Zarmpi et al., 2020); however, only a small number have reported excipient variability for extended release formulations (Ilyes et al., 2021; Kosir et al., 2018; Zhang et al., 2018).

Tablet manufacturing by direct compression represents a cost effective and relatively simple approach for tablet manufacturing, as it comprises a minimal number of process steps (Alderborn and Nystrom, 1996). Although the direct compression process has been used routinely for more than a century, the development and maintenance of robust direct compression processes requires a good knowledge and understanding of the interplay between raw material properties (Worku et al., 2017; Yu et al., 2021b), formulation (Dhondt et al., 2022) and process parameters (de Backere et al., 2022; Grymonpre et al., 2018) to avoid potential problems during manufacturing. Several proposals towards systematic approaches in tablet manufacturing have been made. The Manufacturing Classification System (MCS) (Leane et al., 2015), the compression behavior classification system (Dai et al., 2019) and the process classification maps linking API physical properties and formulation to process parameters (White et al., 2022) were developed and established for guiding and accelerating tablet formulation development by direct compression. Typically, the process of direct compression includes raw material blending, tableting (particle rearrangement, elastic and plastic deformation of particles, fragmentation and formation of interparticulate bonds) and coating (Alderborn and Nystrom, 1996; Carlin, 2008; Lieberman and Lachman, 1989). As the original properties of the raw materials are not significantly modified during the direct compression process, their intrinsic flow and compressibility can be limiting properties. When formulating extended release direct compression tablets, the selection of the right combination of excipients is extremely critical. It must fulfil certain criteria, including adequate density, good powder flow properties and compressibility. There are numerous methods to characterize the tableting behavior of powders. The principal material properties for the characterization of tablet compression are compressibility, tabletability and compactibility, as outlined in the USP <1062> Tablet Compression Characterization. These fundamental concepts capture the relationships among compaction pressure, tablet porosity (ε) or solid fraction, and tablet tensile strength (σ) (USP 40-NF 35, 2017), as illustrated in Fig. 1.

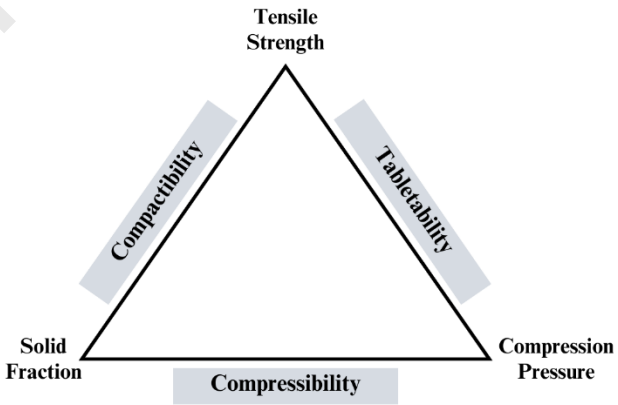

Fig. 1. USP <1062> tablet compression characterization based on the relationships between tensile strength, solid fraction, and compaction pressure.

Since direct compression is highly reliant on API and excipient properties, the mitigation of raw material-induced variability should be considered upstream of tablet manufacturing. Variability in MCC physical (e.g., ρ_{bulk}, ρ_{tapped}, particle size) and flow properties can lead to different tablet mechanical properties (e.g., tensile strength), functionality and manufacturability, thus resulting in undesired tablet quality (Zhao et al., 2022). By exploring and understanding the raw material- and process-related factors, i.e., establishing relationships between CMAs and critical process parameters (CPPs), it is possible to establish and maximize tablet manufacturing process robustness. This approach ensures that the production of tablets meets the required quality standards.

Previous studies attempted to extensively explore raw material properties linking them with direct compression process performance and deploying predictive models for formulation and process development (Bekaert et al., 2021; Escotet-Espinoza et al., 2018; Hayashi et al., 2021; Yu et al., 2021b). Other studies have also correlated raw material and blend properties with the process behavior via multivariate tools at different unit operations of continuous direct compression manufacturing systems (e.g., feeding, die-filling and compression steps) (Bekaert et al., 2021; Van Snick et al., 2018b; Van Snick et al., 2019). Integrated pharmaceutical continuous manufacturing (CM) may be of greater interest due to the potential use of process analytical technology for continuous monitoring of CPPs as well as CQAs of raw materials and final drug products. This leads to reduced production times and handling steps, improving the quality, efficiency and flexibility of manufacturing (Vanhoorne and Vervaet, 2020). Van Snick et al. (2018a) and their coworkers proposed a holistic material characterization approach and developed a multivariate raw material property database of 55 pharmaceutical powders, including a wide variety of APIs and excipients, that were characterized using a wide variety of descriptors. Principal component analysis (PCA) was applied, which allowed the authors to identify the critical material properties and support a rational selection of routine characterization techniques. The developed material database can be key in successful formulation design and predicting how a material behaves at each individual unit operation. Dhondt et al. (2022) developed a data-driven platform linking raw material properties, blend composition and process settings with tablet CQAs using the raw material properties built by Van Snick et al. (2018a). Applying this model, it is possible to improve the development process for new drug products and fine-tune the compaction process settings. Although Van Snick's studies included a high quantity of excipients, some of them used in extended release formulations such as HPC and/or HPMC, these studies were not specifically designed for extended release formulation and did not consider different matrix systems. Additionally, a recent study used PCA to evaluate the behavior of different materials for direct compression. They focused on a wide range of compression descriptors instead of the excipient type (Berkenkemper et al., 2023b).

For extended release formulations, where controlled drug release is critical, accurate control of tablet mechanical properties becomes even more significant to achieve and does not compromise therapeutic efficacy. In the current paper, a holistic approach will be implemented to study and understand how the raw material properties of different extended release formulation-related excipients can impact manufacturability. Fifteen excipients commonly used in extended release formulations, comprising matrix former polymers and diluents, were selected to encompass a wide variety of material properties. The materials selection took into account the combination of their availability, literature review findings and prior knowledge. The compressibility, tabletability and compactibility of the excipients were compared to facilitate their appropriate use in future extended release matrix tablet development. Moreover, the most significant powder

properties and mechanical parameters on tableting feasibility were identified by analyzing data with different multivariate tools.

2. Materials and methods

2.1. Materials

The materials (15) included in this study were purchased from or provided by BASF (Ludwigshafen, Germany), The Dow Chemical Company (Midland, MI, USA), Merck & Co. (Kenilworth, New Jersey, USA), JRS Pharma (Rosenberg, Baden-Wurttemberg, Germany), BENEO (Mannheim, Baden-Wurttemberg, Germany), Avesta Pharma Pvt. Ltd. (Mumbai, Maharashtra, India), Roquette (Lestrem, France), MEGGLE Pharma (Wasserburg am Inn, Germany) and UNDESA (Barcelona, Spain). Table 1 provides an overview of the raw materials. Chemical Abstracts Service (CAS) number and unique ingredient identifier (UNII) were used as identifiers linked to the substance's molecular structure or descriptive information.

163 **Table 1**

164 Raw materials used in the study, their function and manufacturer.

Abbreviation	Excipient name	Commercial name	Function	CAS N.	UNII	Manufacturer
KL-SR	Acetate polyvinyl 80% PVP 20%	Kollidon® SR	Matrix former	9003-20-7 9003-39-8	32K497ZK2U	BASF
HPMCK4M	Hydroxypropyl methylcellulose	Methocel™ K4M Premium	Matrix former	9004-65-3	3NXW29V3WO	DuPont
HPMCK100	Hydroxypropyl methylcellulose	Methocel™ K100 Premium CR	Matrix former	9004-65-3	3NXW29V3WO	DuPont
PEO-N750	Poly(ethylene)oxide	POLYOX™ WSR N750	Matrix former	25322-68-3	4QIB4U4CQR	DuPont
PEO-1105	Poly(ethylene)oxide	POLYOX™ WSR 1105	Matrix former	25322-68-3	16P9295IIL	DuPont
PEO-303	Poly(ethylene)oxide	POLYOX™ WSR 303	Matrix former	25322-68-3	G3MS6M810Y	DuPont
PVA	Polyvinyl alcohol	Parteck® SRP80	Matrix former	9002-89-5	532B59J990	Merck & Co.
RL	Lactose coprocessed	RetaLac®	Matrix former	5989-81-1 9004-65-3	EWQ57Q8I5X 39J80LT57T	MEGGLE
ADCP	Calcium hydrogen phosphate anhydrous	Emcompress® Anhydrous	Diluent	7757-93-9	L11K75P92J	JRS Pharma
G721	Isomalt	galenIQ™ 721	Diluent	64519-82-0	S870P55O2W	BENEO
TA-80	Lactose Monohydrate	Tablettose® 80	Diluent	64044-51-5	EWQ57Q8I5X	MEGGLE

MD-IT12	Maltodextrin	Glucidex® IT 12	Diluent	9050-36-6	7CVR7L4A2D	Roquette
MAN-400DC	Mannitol	Pearlitol® 400 DC	Diluent	69-65-8	3OWL53L36A	Roquette
PEG6000	Poly(ethylene glycol) 6000	Macrogol 6000	Diluent	25322-68-3	30IQX730WE	Avesta Pharma
SMCCHD90	Silicified Microcrystalline Cellulose	PROSOLV® SMCC HD90	Diluent	9004-34-6	OP1R32D61U	JRS Pharma
MgSt	Magnesium stearate	Kemilub EM-F-V	Lubricant	557-04-0	70097M6I30	UNDESA

2.2. *Methods*

2.2.1. *Macroscopic material characterization methods*

2.2.1.1. *Laser diffraction*

Particle size distribution (PSD) of the raw material samples was performed by laser diffraction using a Horiba LA-960v2 Particle Size Analyzer - dry module. The powder was fed by a vibratory feeder to the dry cell of the light scattering instrument. Automatic control of the sample feed rate was set with an air pressure of 0.20 MPa, and each sample was measured in triplicate. A refractive index of 1.51 and transmittance range of 98.0%-95.0% (target T%=97.0%) were chosen. The statistical data were analyzed via Horiba LA-960 software. For each volumetric distribution, the 10th, 50th and 90th quantiles were reported as Dv10, Dv50 and Dv90, respectively. The width (dwidth) and span (dspan) were calculated to describe the PSD according to Eqs. (1) and (2):

$$dwidth = Dv90 - Dv10 \quad (1)$$

$$dspan = \frac{dwidth}{Dv50} \quad (2)$$

2.2.1.2. *Powder density and flow properties*

True density is a critical material attribute of powder materials since it is used to estimate tablet porosity and consequently compressibility and compactibility. The true density (ρtrue) of each excipient was measured using a helium pycnometer (AccuPyc 1330, Micromeritics®, USA). The measurements were performed with a cell of 10 cm^3 at an equilibrium rate of 0.005 psig/min and a gas input pressure of 19.5 psi. The sample chamber was purged with 10 purging cycles followed by 5 measurement cycles. The true

density (g/cm^3) was determined by dividing the sample weight by the volume. The bulk (ρ_{bulk}) and tapped density (ρ_{tapped}) of the powder particles were determined in accordance with Ph.Eur. 2.9.3, using a 100 mL graduated cylinder mounted on a tapping device (Erweka SVM, Tapped Density Tester, Heusenstamm, Germany). An exact mass of powder was gently poured into the graduated cylinder. The initial volume and volume after 1250 taps were recorded to calculate the ρ_{bulk} and ρ_{tapped}, respectively. The flow properties of the powder were evaluated from the Hausner ratio (HR) and compressibility index (CI). HR and CI were calculated according to Eqs. (3) and (4), respectively:

$$HR = \frac{\rho_{tapped}}{\rho_{bulk}} \quad (3)$$

$$CI\ (\%) = 100\ x \left(\frac{\rho_{tapped} - \rho_{bulk}}{\rho_{tapped}}\right) \quad (4)$$

2.2.1.3. Flow rate

The flow rate (FR) of the powder was determined using a granulate flow tester (GTB, Erweka, Germany) with an 11.3 mm nozzle and a stirrer setting of 2. Approximately 30 g of material was poured into the 200 mL hopper. Material was allowed to flow through the funnel orifice, and the flow rate was determined as the ratio of weight (g) to time (seconds). The mean of three determinations was recorded.

2.2.1.4. Angle of repose

The flow properties of powder samples were assessed (in triplicate) by measuring the angle of repose (AR) using a granulate flow tester (GTB, Erweka, Germany). The powder (20 g) was poured into the funnel and allowed to flow through the hopper with a 10 mm orifice diameter, forming a cone of powder. The sidewall of the built-up cone was measured using an automatic laser, and the actual angle of repose was calculated.

2.2.1.5. Moisture gain

For determination of the moisture gain (MG) (%), the powder samples were taken in separate Petri dishes and placed in a desiccator exposed at a temperature of 22 ± 2°C with a relative humidity of approximately 75 ± 2%. After 24 h, the percentage mass gained by the samples was calculated.

2.2.2. Powder compression

Tablets were prepared by direct compression of lubricated excipients. All excipients were manually passed through a sieve with a mesh size of 850 µm. Each excipient was lubricated with 1% w/w of magnesium stearate, previously sieved through a 250 µm mesh. To expedite the tableting process, a total of 20 g of each blend was mixed in a 75 mL HDPE wide-mouth bottle using a high-frequency agitator, CryoMill (Retsch), for 1 minute at 30 Hz. The compaction behavior of powder blends was evaluated using a single-station compaction simulator (STYL'One Classic, Medel'Pharm, France). The simulator

was operated in displacement mode to simulate a S rotary press-TSM D compaction cycle with a pitch circle diameter of the turret of 370 mm. The compaction simulator was tooled with a standard EU-D 11.28 mm round flat-faced punch and die. To enhance the accuracy of the measurements, the impact of machine deformation was taken into consideration through the compression of an 11.3 mm stainless steel disk. Samples were prepared by manually pouring the weighed respective amount of powder (450 mg ± 5% range) into the die, and a five-point compression profile was made from 25 MPa to 300 MPa. For PEO polymers, an additional shorter study was performed to a range of 25 MPa to 100 MPa to better characterize their tabletability and compactibility behavior (Al-Nasassrah et al., 1998; Yu et al., 2021a). To evaluate the dependence on compression speed, the powders were compressed at simulated compression speeds of 2 rpm and 80 rpm, corresponding to dwell times of 180-930 ms and 5-14 ms (time interval of 90% of force), respectively, depending on the excipient deformation behavior.

2.2.3. Tablet characterization

After ejection and a 24-hour relaxation period, the tablet thickness, diameter, crushing force, and weight were determined using a tablet tester (Smart-Test50, Sotax AG, Switzerland).

2.2.3.1. Tensile strength

Tensile strength (σ) constitutes a fundamental property of a compact and provides extremely useful information, as tablet crushing force is applicable to a single tablet size and shape. The tablet tensile strength (MPa) was calculated by Eq. (5) (Fell and Newton, 1970), where F, d and T denote the crushing force (N), tablet diameter (mm) and tablet thickness (mm), respectively.

$$\sigma = \frac{2F}{\pi dT} \tag{5}$$

2.2.3.2. Porosity

The tablet porosity (ε), as a descriptor of the structure of the compact or state of consolidation, was calculated by using the out-of-die characterization of the tablets according to Eq. (6):

$$\varepsilon = 1 - \frac{\rho_{tablet}}{\rho_{true}} x100 \tag{6}$$

where ρ_{tablet} denotes the apparent tablet density (g/mL), which was calculated by dividing the tablet mass by its volume. The solid fraction is the inverse of the porosity.

2.2.3.3. Mechanical properties

To gain a thorough qualitative understanding of the compression behavior of the studied formulations, plots illustrating compressibility, compactibility, and tabletability were generated. Simultaneously, with the purpose of finding quantitative variables to

incorporate into PCA, some descriptors were assessed by widely used mathematical models.

2.2.3.3.1. Compressibility

The compressibility of a material denotes the effect of compression pressure on the porosity of compacts, i.e., how readily the material undergoes a change in volume (Sun, 2016). For describing tablet compressibility, different compression equations have been proposed (Berkenkemper et al., 2023a). Of the several equations, the relationship developed by Heckel (1961), which is based on the assumption that the porosity of the tablet decreases with increasing pressure and follows first-order kinetics, is one of the most well-known mathematical models. The Heckel analysis has been criticized due to its known limitations, namely, the sensitivity to the true density, material deformation behavior and experimental compaction conditions (Rue and Rees, 1978; Sonnergaard, 1999). Although it is the most established and widely used method for describing material compressibility through its plasticity (Vreeman and Sun, 2021), it should be noted that a binary approach classifying materials as brittle/ductile based on a single material parameter can be insufficient, and a holistic approach should be applied considering potential alternative mechanical metrics (Yost et al., 2022). Heckel analysis can be applied either as an in-die or out-of-die method; however, the in-die method was found to be a robust analysis, providing more accurate and reliable results (Berkenkemper and Kleinebudde, 2022; Vreeman and Sun, 2021). The compression parameter derived from Heckel analysis that indicates the plasticity of the material is the yield pressure (P_y), calculated from Eq. (7):

$$-\ln(\varepsilon) = \frac{1}{P_y}P + \alpha \tag{7}$$

where ε is the porosity of the tablet, P_y^{-1} is the slope of the linear portion of the Heckel plot, P is the compression pressure, and α is the y-axis intercept. The Heckel equation was fitted using data collected from in-die compaction at a maximum compaction pressure of 300 MPa. Porosity was calculated using the in-die tablet thickness measured by the displacement sensors of the compaction simulator, the true density and the out-of-die tablet weight. The Py was determined by linear regression of the linear region of the Heckel plot using Analis software (Medelpharm, France). Qualitative assessment was performed to select the most central part of the linear region with a coefficient of determination set to at least 0.99.

2.2.3.3.2. Tabletability

A tabletability plot has been defined as a powdered material's ability to be transformed into a tablet of a specific strength under a specific compression pressure (Sun, 2016). A recent equation was proposed by Vreeman and Sun (2022b) to describe the tabletability of powders, i.e., the cause–effect relationship between the tablet tensile strength and the applied compression pressure. The equation derived from the Ryshkewitch and Kuentz-Leuenberger equations describes an asymmetric sigmoidal function and contains three fitting constants (α, β and σ_{max}) and the Lambert W function. Similarly, the Gompertz function is also an asymmetric sigmoidal function that models exponential growth. A comparison between these two equations in fitting tabletability data was accessed.

Despite the superiority of the new equation for realistically describing tabletability, Gompertz fittings are highly correlated with plasticity parameters (Vreeman and Sun, 2022b). The tabletability data were fitted by the 3P Gompertz function according to Eq. (8):

$$TS = y_{max} e^{-e^{-b(P-c)}} \quad (8)$$

where y_{max} is the asymptotic value as the compression pressure (P) approaches infinity, b is a growth constant rate and c is the inflection point at the center of the curve where the convex curve becomes concave.

2.2.3.3.3. Compactibility

Compactability describes the intrinsic relationship between tablet tensile strength and solid fraction and is related to the binding force between the particles as the compression pressure increases (Osamura et al., 2016). Typically, tablet tensile strength increases exponentially with solid fraction, as the increases in interparticle bonding strengthen a compact. The compactibility profiles of the investigated excipients were plotted by fitting the out-of-die porosity and tensile strength according to the Ryshkewitch-Duckworth equation (Duckworth, 1953):

$$ln(\sigma) = \sigma_0 - k_b \varepsilon \quad (9)$$

where σ is the tensile strength of the compact, ε is the porosity of the compacts, σ_0 is the theoretical maximal tensile strength of the compact at zero porosity, and k_b is the slope of the linear regression which represents the bonding capacity of the powder particles under increasing pressure. The values of the compactibility parameter (σ_0) and bonding capacity (k_b) obtained using the Ryshkewitch-Duckworth equation were determined for all studied excipients.

2.2.4. Compression analysis

2.2.4.1. Plastic and compression energy

Compression energy (Ec) is the energy given to the tablet during the compression phase when the compression force increases. The elastic energy (Ep) is the energy recovered from the tablet when the compression force decreases. Its value is reported negatively since the elastic recovery direction is opposite to the direction of the compaction force. Plastic energy is related to irreversible compression (e.g., plastic deformation) and corresponds to the sum of compression energy and elastic energy (Bourduche et al., 2020; Garekani et al., 2001). Compaction raw data were produced, and Ec and Ep were automatically obtained according to the recorded force–displacement curve by the data acquisition software (Analis®, 2.08.5, Medelpharm, France).

2.2.4.2. In-die elastic recovery

In the initial compaction phase, the particles can undergo plastic and elastic deformation. When the compaction force is unloaded, the elastic deformation is recovered. During the

decompression phase, many powders undergo elastic recovery, resulting in axial and radial expansion of the tablet (Picker, 2001). Excessive elastic recovery is prone to manufacturing defects, particularly capping (Vreeman and Sun, 2022a). Therefore, using elastic recovery as a key parameter for predicting the tendency of formulation to capping during drug product development would be a helpful approach from a pharmaceutical industry perspective to prevent future issues during the scale-up (Meynard et al., 2022b). The in-die elastic recovery (ER) of the tablets is defined as the percent increase in in-die tablet thickness when the axial pressure changes from the maximum value to zero. It is determined using Eq. (10), according to the method introduced by Armstrong and Hainesnu.Rf (1974).

$$ER\ (\%) = \frac{h_t - h_0}{h_0} x100 \qquad (10)$$

where h_0 is the corrected compression thickness at the maximum compression force (mm) and h_t is the in-die recovery thickness (mm). i.e., the distance between the punches when the force on the upper punch decreases to zero. The corrected compression thickness at maximum force is the exact value of the tablet thickness at maximum compression force after correcting for punch and machine deformation.

2.2.4.3. Ejection stress

The tablet ejection force is the force required to eject the tablet from a die after compression. It is mainly governed by the constraint of compact-die wall stress. The tablet ejection stress is the product of the compact-die wall friction coefficient and the residual die wall force stress upon tablet ejection. The ejection stress is calculated from the ejection force to account for the punch and die geometries. A higher ejection force is predicted for high radial die wall stress and can be associated with tablet defects such as capping and lamination (Uzondu et al., 2018). The ejection stress (MPa) is obtained from its maximum ejection force (EF), tablet diameter (d) and tablet thickness (T) as described in Eq. (11). The ejection force was measured and recorded during the compaction process with STYL'One Classic and Analis Software (Medelpharm, France).

$$Ejection\ stress = \frac{EF}{\pi dT} \qquad (11)$$

2.2.4.4. Strain-rate sensitivity

The strain rate sensitivity (SRS) measures the impact of the consolidation time and tableting speed on the deformation behavior of a material (Roberts and Rowe, 1985). The SRS of numerous pharmaceutical materials can directly affect the mechanical strength of tablets and subsequently impact the product quality attributes (Roopwani and Buckner, 2021). A tabletability plot for each excipient and compression speed was fitted with a Gompertz exponential function. A predicted tensile strength at a pressure of 150 MPa was used to evaluate the differences between tensile strength obtained at fast (σ_{fast}) and slow (σ_{slow}) compression speeds was normalized to tensile strength at slow compression speed using Eq. (12) For PEO polymers, the SRS was determined at 50 MPa.

$$SRS\ (\%) = \frac{\sigma_{fast} - \sigma_{slow}}{\sigma_{slow}} x100 \quad (12)$$

2.2.5. Data analysis

Data were analyzed via JMP® 17 (SAS Institute Inc., NC, USA) statistical analysis software. Different statistical techniques were performed, such as distribution, scatterplot matrix and PCA.

2.2.5.1. Multivariate analysis

PCA is a multivariate data analysis method used for reducing the dimensionality of a dataset. PCA orthogonally transforms a high-dimensional set of observations of possibly correlated variables into a new set of uncorrelated variables called principal components (PCs). By reducing the dimensionality of the data, PCA can help to identify the most important variables, key patterns, and relationships in a dataset. The first principal component captures the most variance in the data, while each subsequent component explains the next most variance, subject to being orthogonal to the previous components. In the case of oral extended release delivery systems, PCA can potentially be used to identify, evaluate and optimize input factors such as formulation or manufacturing process variables that can affect drug product CQAs (Sousa et al., 2022).

3. Results and discussion

3.1. Raw material physical attributes

The physical properties of the excipients were studied, including Dv10, Dv50, Dv90, dspan, dwidth, ρ_{true}, ρ_{bulk}, ρ_{tapped}, FR, AR, CI, HR and MG. The volume-weighted PSD of the investigated excipients is presented in Fig. 2. Most of the PSD curves exhibit a mono-modal distribution, although slight differences in the shape of the PSD curve are observed among the excipients. KL-SR, HPMCK4M, HPMCK100 and PVA had similar PSDs, representing smaller particle sizes covering a range of median particle sizes from 57.63 µm to 74.95 µm. Powders with smaller particle sizes are more likely to be cohesive and form aggregates, resulting in powder flow issues (Allenspach et al., 2020). In contrast, MAN-400DC showed a larger particle size, with a median particle size value of 393.17 µm. The PSD expressed in span are in the range of 1.06 to 2.90. A lower span value indicates a narrow particle size distribution and usually contributes to blend homogeneity. HPMCK4M had the highest span value (2.90), which can potentially lead to segregation during tablet compression and, consequently, weight variability and poor content uniformity.

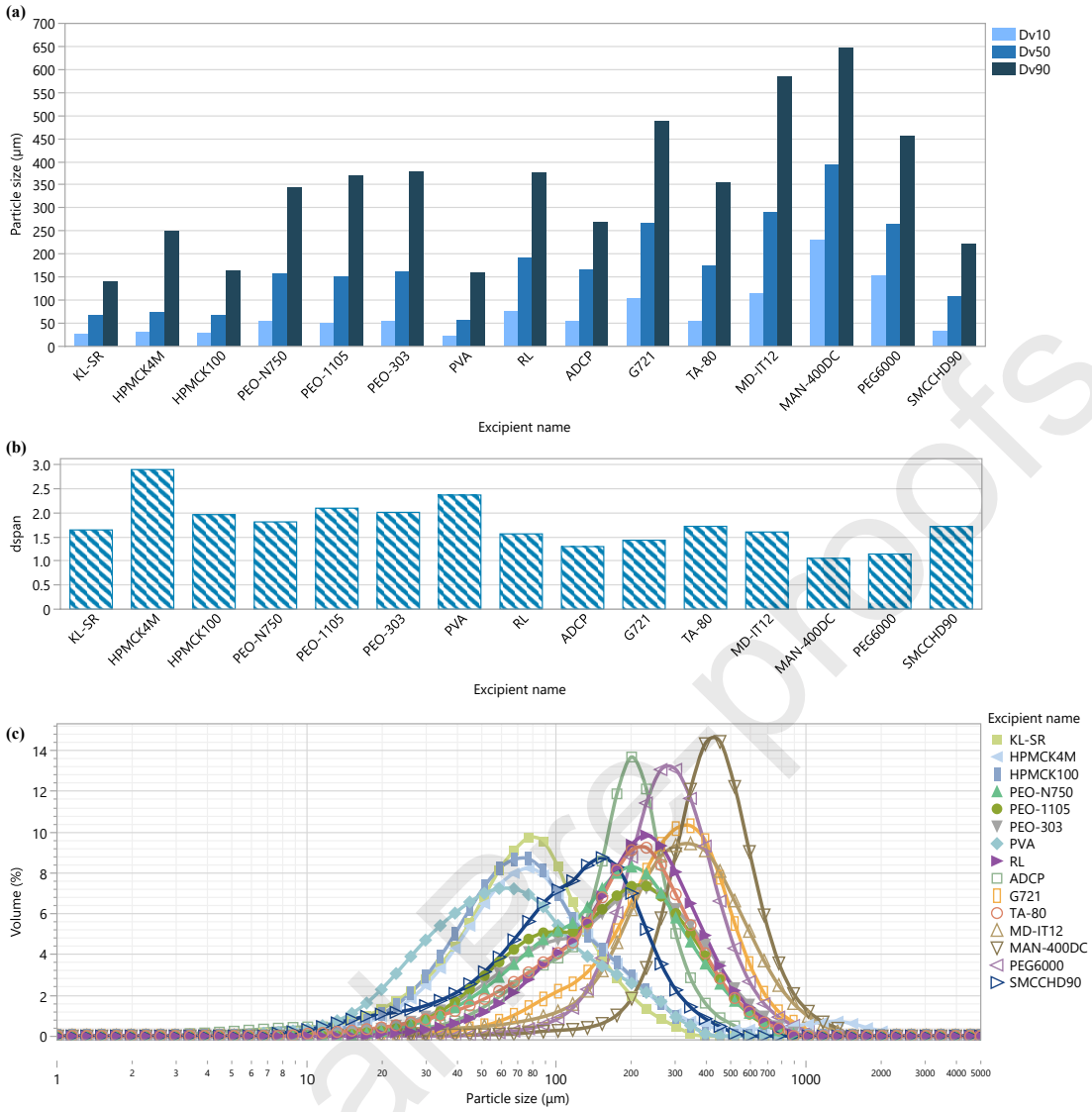

Fig. 2. Particle size analysis of the excipients: percentile values of Dv10, Dv50 and Dv90 (a), dspan (b) and particle size distribution (c).

It is generally known that flow behavior can significantly affect the direct compression process as well as the CQAs of the drug product (e.g., weight and content uniformity). Accordingly, the density and flow properties of the excipients were examined, and a comprehensive overview of the obtained results is shown in Table 2. The bulk density of all excipients ranged between 0.274-0.720 g/cm^3. The ρ_{tapped} was calculated and found to be between 0.371-0.844 g/cm^3. ACDP, MAN-400DC and TA-80 exhibited the highest values of both ρ_{bulk} and ρ_{tapped}, while the lowest values were observed for RL, HPMCK4M, HPMCK100, MD-IT12 and KL-SR. The CI and HR were calculated from the ρ_{bulk} and ρ_{tapped}. Empirically, higher CI (> 25%) and HR (<1.34) values mean that the material is more cohesive and less able to flow freely. A CI of less than 15% and an HR of less than 1.18 have been used to indicate good flow properties since particles show little potential for further consolidation. The CI was found to be between 9.14 and 31.89% for all excipients. Similarly, HR values were noted in the range of 1.10 and 1.47. Almost all diluents showed CI and HR values lower than 15% and 1.20, respectively, indicating good compressibility properties. Otherwise, there is a substantial dispersion of CI and HR values in the case of polymers. According to the values shown in Table 2, good flow

properties were obtained for PEOs (PEO N-750, PEO-1105 and PEO-303) and KL-SR powders in this study. HPMCK4M, HPMCK100 and PVA showed the highest values of CI and HR. Grdesic et al. (2020) characterized the flow and compaction properties of different grades and suppliers of HPMC (type 2208), including K4M and K100M CR. The CI and HR values, even after the addition of magnesium stearate, showed poor to very poor flow properties. RL, a spray-dried coprocessed 50:50 HPMC:lactose blend, shows an intermediate flow with values of 25% for CI and 1.33 for HR, similar to the literature data (Cirin-Varadan et al., 2022).

A powder with good flow properties generally has a higher FR and lower AR. AR is an indirect method of qualifying powder flow properties because of its relationship with interparticle cohesion. According to the USP, an AR value less than 40° is a direct indicator of satisfactory powder flow properties. MAN-400DC, PEG6000 and ADCP exhibited higher FR values (16.858, 15.307 and 15.152 g/s, respectively) and lower AR values, as expected due to their high ρ_{bulk} and ρ_{tapped}. The larger particle size of MAN-400DC supports its superior free powder flow. HPMCK4M, HPMCK100 and PVA had poor free flow through the orifice with AR values above 40°. These results can explain the deterioration of the flow properties of extended release formulations with increasing additions of PVA (Muzikova et al., 2018).

Table 2

Raw material physical attributes of the excipients. Average values are shown ± standard deviation ($\bar{x}$ ± SD).

Excipient	ρ_{true} [g/cm³]	ρ_{bulk} [g/cm³]	ρ_{tapped} [g/cm³]	CI (%)	HR	FR [g/s]	AR [°]	MG (%)
KL-SR	1.227 (0.002)	0.388 (0.000)	0.447 (0.000)	13.25	1.15	2.887 (0.082)	25.533 (0.094)	0.539
HPMCK4M	1.336 (0.001)	0.323 (0.001)	0.469 (0.003)	31.09	1.45	3.271 (0.144)	40.433 (1.969)	0.692
HPMCK100	1.341 (0.000)	0.325 (0.004)	0.477 (0.004)	31.89	1.47	3.278 (0.096)	41.200 (0.980)	0.712
PEO-N750	1.251 (0.000)	0.413 (0.001)	0.462 (0.004)	10.62	1.12	9.036 (0.039)	16.667 (0.793)	0.090
PEO-1105	1.251 (0.001)	0.455 (0.003)	0.512 (0.004)	11.22	1.13	9.129 (0.306)	18.500 (0.216)	0.094

PEO-303	1.248 (0.000)	0.467 (0.003)	0.514 (0.005)	9.14	1.10	8.572 (0.069)	15.067 (0.736)	0.108
PVA	1.293 (0.000)	0.532 (0.000)	0.693 (0.006)	23.33	1.30	1.775 (0.071)	40.433 (1.461)	0.432
RL	1.449 (0.000)	0.274 (0.000)	0.371 (0.005)	26.03	1.35	6.188 (0.126)	30.667 (0.525)	0.341
ADCP	2.804 (0.003)	0.720 (0.003)	0.844 (0.001)	14.62	1.17	15.152 (0.000)	23.000 (0.707)	0.074
G721	1.498 (0.000)	0.411 (0.004)	0.475 (0.001)	13.54	1.16	9.840 (0.200)	23.533 (0.262)	0.027
TA-80	1.532 (0.001)	0.615 (0.007)	0.707 (0.001)	13.09	1.15	10.870 (0.096)	27.233 (0.918)	0.003
MD-IT12	1.366 (0.001)	0.361 (0.004)	0.425 (0.002)	14.89	1.18	7.774 (0.115)	29.333 (0.170)	0.460
MAN-400DC	1.492 (0.000)	0.658 (0.001)	0.776 (0.002)	15.27	1.18	16.858 (0.271)	21.800 (0.779)	0.023
PEG6000	1.242 (0.000)	0.544 (0.003)	0.615 (0.000)	11.65	1.13	15.307 (0.110)	22.467 (0.655)	0.048
SMCCHD90	1.555 (0.000)	0.446 (0.002)	0.526 (0.003)	15.20	1.18	5.553 (0.210)	21.467 (0.939)	0.199

3.2. *Mechanical properties*

The mechanical properties of the extended release formulation-based excipients were evaluated by comparing their compressibility, tabletability and compactibility. The profiles are shown in Fig. 3, and the parameters derived from the applied mathematical models are described in Table 3. The analysis was conducted at a speed of 80 rpm, mimicking the high speed of industrial-scale rotary tablet presses in commercial manufacturing. The compressibility plots are depicted in Fig. 3a. There was no large

difference in the compressibility profiles among the excipients. Two stages can be observed in the plot: an initial consolidation stage where the solid fraction increases almost linearly with compaction pressure up to a solid fraction of approximately 0.8 and a second stage where the tablet's solid fraction tends to achieve constant values, despite the increasing compaction pressure. At this stage, the particles are forced to fill the void spaces, resulting in no observed increase in the solid fraction. In general, higher solid fraction values were obtained for diluents compared to polymers. ADCP is very difficult to densify below a porosity of 0.3, even at the highest compaction pressure of 300 MPa in this study, exhibiting the least reduction in porosity compared to the other diluents. Additionally, ADCP and G721 show very poor plasticity and low compressibility properties based on their high Py. On the other hand, the lowest Py of PEG6000 (15.5 MPa) indicates that less force is required to form a compact. PEG6000 exhibited a plastic deformation, being more compressible and easier to form into a tablet. The molecular weight (MW) and amount of PEG6000 can have a significant impact on tablet formulation compressibility. Generally, lower PEG MW grades and higher concentrations tend to have better compressibility (Larhrib and Wells, 1998). Among polymers, PEOs have the highest solid fraction upon application of the lowest compaction pressure. The compressibility profiles of PEOs with different molecular weights appeared to undergo volume reduction to a similar extent, as described by (Yu et al., 2021a). The extent of reduction in porosity did not appear to differ significantly between HPMCK4M, HPMCK100, KL-SR and RL. The steep slope observed for these polymers' plots at the lower compaction pressure values suggests lower resistance to volume reduction, possibly correlated with their lower bulk density values compared to PEO polymers. It should be noted that it was not possible to determine the solid fraction of PVA at lower compaction pressures due to its weak structural integrity.

The tabletability (Fig. 3b) of the excipients at 150 MPa follows the order KL-SR> SMCCHD90 > G721 = HPMCK100 > HPMCK4M > MD-IT12 > RL > ADCP = MAN-400DC > TA-80 > PVA > PEG6000. SMCCHD90 and KL-SR compacts showed the highest increase in tensile strength of 9 MPa up to a compaction pressure of 200 MPa. The steep increase in tensile strength at lower compaction pressure (e.g., 50 MPa) is due to reduced tablet porosity caused by particle rearrangements and volume reduction, resulting in an increased bonding area. This behavior is typically seen with plastic deforming materials (Hentzschel et al., 2012). PEO polymers also seem to have good tabletability behavior with tensile strength values higher than 2 MPa and higher values of growth rate (b). As a general rule of thumb, 1.7 – 2.0 MPa is considered the minimum value of tensile strength to obtain mechanically strong tablets to withstand commercial manufacture and packaging (Pitt and Heasley, 2013). However, the high degree of plastic deformation of PEO (Yang et al., 1996) polymers, characterized by their ability to deform permanently, makes it impossible to determine the tablet resistance to crushing at lower porosity values, as the compact deformed (volume reduction) instead of failed in tension (Al-Nasassrah et al., 1998; Podczeck, 2012), exceeding the measuring range of the hardness tester (maximum 800 N). Therefore, the tabletability and compactibility plots of PEO polymers are produced below 100 MPa of compression pressure. Comparing the tabletability profiles of both HPMC, HPMCK100 shows superior tabletability, as reported by Grdesic et al. (2020). Additionally, particle size and moisture content have been shown to affect the mechanical strength of tablets. A small particle size of plastically deformed materials allows for a high surface area for bonding, resulting in increased tensile strength at lower compression pressure. However, at higher values of compression pressure (> 150 MPa), the tensile strength of both HPMCs reaches a plateau, assuming an asymptotic

514 profile. This behavior can be explained by the high moisture content values present in
515 HPMC polymers that may have a plasticizer effect. Therefore, the tensile strength reaches
516 a maximum and may start decreasing. The choice of HPMC grades significantly impacts
517 tabletability and compactibility profiles, with higher degrees of substitution leading to
518 improved tabletability and compactibility due to an increased number of contact points
519 between particles in the matrix tablet (Ghori, 2016). On the other hand, PVA and
520 PEG6000 exhibit poorer tabletability, as evidenced by lower values of the Gompertz
521 function asymptote (c). Even under high compression pressures, the tensile strength
522 remains below 2.0 MPa.

523 The compactibility profiles are shown in Fig. 3c and Table 3. Except for ADCP, at a solid
524 fraction of 0.8, the compactibility profile was ranked in a similar order to the tabletability
525 profile. For all investigated excipients, the compactibility profiles can be well described
526 using the Ryshkewitch-Duckworth parameters ($\sigma 0$ and k_b). The correlation coefficients
527 (R^2) of the Ryshkewitch-Duckworth equation, obtained using nonlinear regression
528 analysis, were above 0.999, exhibiting a good correlation between the tensile strength and
529 compact porosity. ADCP yielded the highest value of the compactibility parameter, $\sigma 0$,
530 of 459.591 MPa, which decreased significantly to 1.175 MPa in the case of PEG6000.
531 The value of k_b follows the order TA-80 > ADCP > PVA > MAN-400DC > RL > PEO-
532 1105 > G721 > PEO N-750 > PEO-303 > HPMCK100 > KL-SR > HPMCK4M >
533 PEG6000 > MD-IT12 > SMCCHD90. Higher k_b values suggest a stronger bonding
534 capacity between the particles, implying a rapid increase in tablet tensile strength with
535 decreasing porosity.

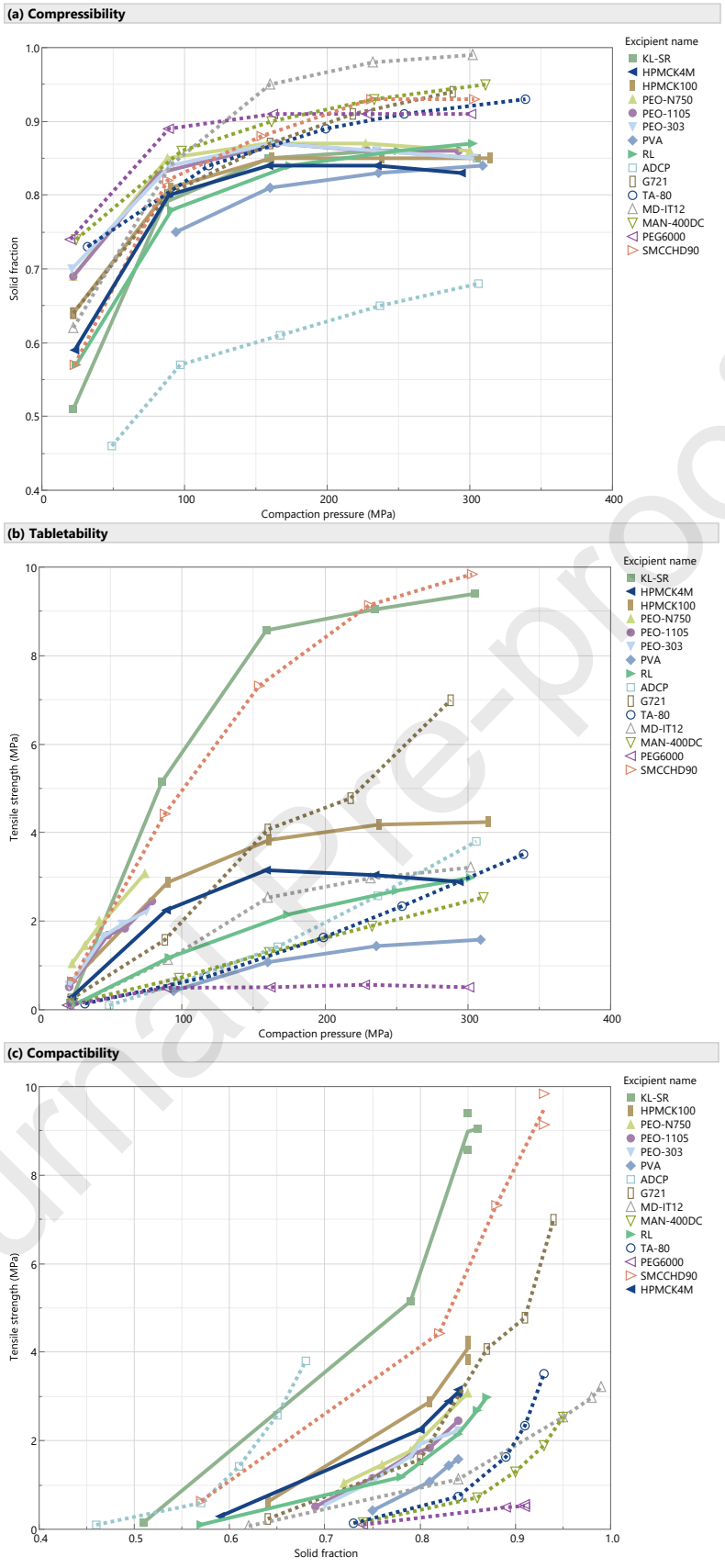

Fig. 3. Compressibility (a), tabletability (b) and compactibility (c) profiles of the investigated excipients at 80 rpm. The solid lines and markers represent the polymers and the open markers and dashed lines represent the diluents.

Table 3

Model parameters and R^2 values for the fit of the compression data at 80 rpm according to Heckel, Gompertz and Ryshkewitch-Duckworth equations.

Excipient	Compressibility - Heckel equation		Tabletability Gompertz function				Compactibility Ryshkewitch-Duckworth equation		
	Py (MPa)	R^2	α	b	c	R^2	σ_0 (MPa)	k_b	R^2
KL-SR	53.4	0.991	9.250	0.029	67.765	0.999	32.379	8.748	0.999
HPMCK4M	53.0	0.993	3.046	0.033	50.179	0.989	12.664	8.747	1.000
HPMCK100	56.3	0.991	4.221	0.023	49.742	0.999	15.541	8.903	1.000
PEO-N750	46.7	0.990	4.212	0.029	34.323	0.987	12.530	9.272	1.000
PEO-1105	44.4	0.993	2.891	0.038	34.390	0.984	11.662	9.617	1.000
PEO-303	42.4	0.994	2.386	0.055	28.073	0.998	10.474	9.181	1.000
PVA	91.2	0.991	1.623	0.018	110.545	1.000	15.739	14.218	1.000
RL	63.3	0.994	3.078	0.014	94.397	0.994	11.666	10.500	1.000
ADCP	706.7	0.998	7.109	0.007	237.648	0.998	459.591	14.934	1.000
G721	817.0	0.995	9.152	0.009	150.364	0.983	3.487	9.609	1.000
TA-80	170.9	0.998	6.653	0.006	260.027	1.000	12.526	18.342	1.000
MD-IT12	817	0.995	3.224	0.020	91.874	0.999	3.487	7.208	1.000
MAN-400DC	148	0.999	3.450	0.008	160.358	0.998	5.027	13.736	1.000
PEG6000	15.5	0.991	0.528	0.047	30.411	0.985	1.175	8.693	1.000

SMCCHD90	66.6	0.995	9.976	0.017	78.712	0.998	15.341	6.697	1.000

3.3. *Relationships among powder and compression descriptors*

The evaluation of the behavior of various powders under compaction pressure involved the determination of a large number of descriptors representing the bulk properties of powder excipients, compression process and tablet attributes. This study provides a complete dataset, presented in Supplementary Material. The relationship between the measured variables from the above experiments can be investigated by performing a correlation analysis on a one-to-one basis using a scatterplot matrix. It should be noted that correlating flow properties of excipients with their plastic deformation during tablet process can provide significant challenges. This may be attributable to multivariate factors impacting the compressibility behavior. A preliminary analysis was performed to assess the main correlations between the studied variables. Among the parameters included in the analysis, those that are theoretically correlated with each other (e.g., Dv10, Dv50, Dv90) and those whose correlation coefficient was between -0.6 and 0.6 were excluded. Fig. 4 shows the scatterplot matrix of the experimental data at 80 rpm customized with density ellipses and significance circles. The ellipses show a 95% bivariate normal confidence density ellipse in each scatterplot. The blue significance circles show the correlations, with dark blue indicating a strong positive relationship between the pairwise variables. Each marker represents one excipient at a given compression pressure.

Some powder bulk physical properties were mutually correlated. Dv50 is negatively correlated with dspan and positively correlated with FR. A negative correlation between Dv50 and dspan indicates that larger particles tend to have a narrower distribution, resulting in a smaller dspan. FR exhibits a positive correlation with Dv50 and ρ_{bulk} and, as expected, a strong negative correlation with AR, CI and MG. Moisture can lead to agglomeration or cohesive behavior between particles, decreasing the flow properties. A positive correlation between FR, Dv50 and ρ_{bulk} suggests that powders with higher density and median particle size tend to have better flow properties. The specific surface area decreases with increasing particle size, resulting in improved flow properties.

Correlations between powder attributes and compression-related descriptors were also found. Plastic (E_p) and compression energy (E_c) showed a positive correlation with compression pression (P) and tensile strength (σ). The E_p of a material is related to its ability to undergo plastic deformation, which is an irreversible change during decompression. In reality, higher compression pressures can result in higher plastic energy absorption, as depicted by a typical stress–strain curve.

High correlations were also observed between ER and flow-related parameters (FR, AR and CI). While these are interrelated parameters that reflect how the physical properties of the powder can influence the tablet compression process, they are typically evaluated independently. ER integrates the elastic expansion of the tablet during the decompression phase and should be minimized to avoid manufacturing defects such as capping. A relationship was also observed between the compactibility descriptors derived from the Ryshkewitch-Duckworth equation (k_b and σ_0) and the density parameters. The density ellipse relating ρ_{true} and σ_0 is narrow and has a steep slope, suggesting a strong correlation between these variables. Compactibility, which describes tensile strength as a function of

solid fraction, suggests that materials with higher ρ_{true} may have stronger interparticle bonds, resulting in higher tensile strength. It is worth noting that while several powder and tablet attributes were shown to be correlated with each other, in some cases, no significant correlations were observed, justifying the diverse set of excipient bulk and mechanical properties provided by the dataset.

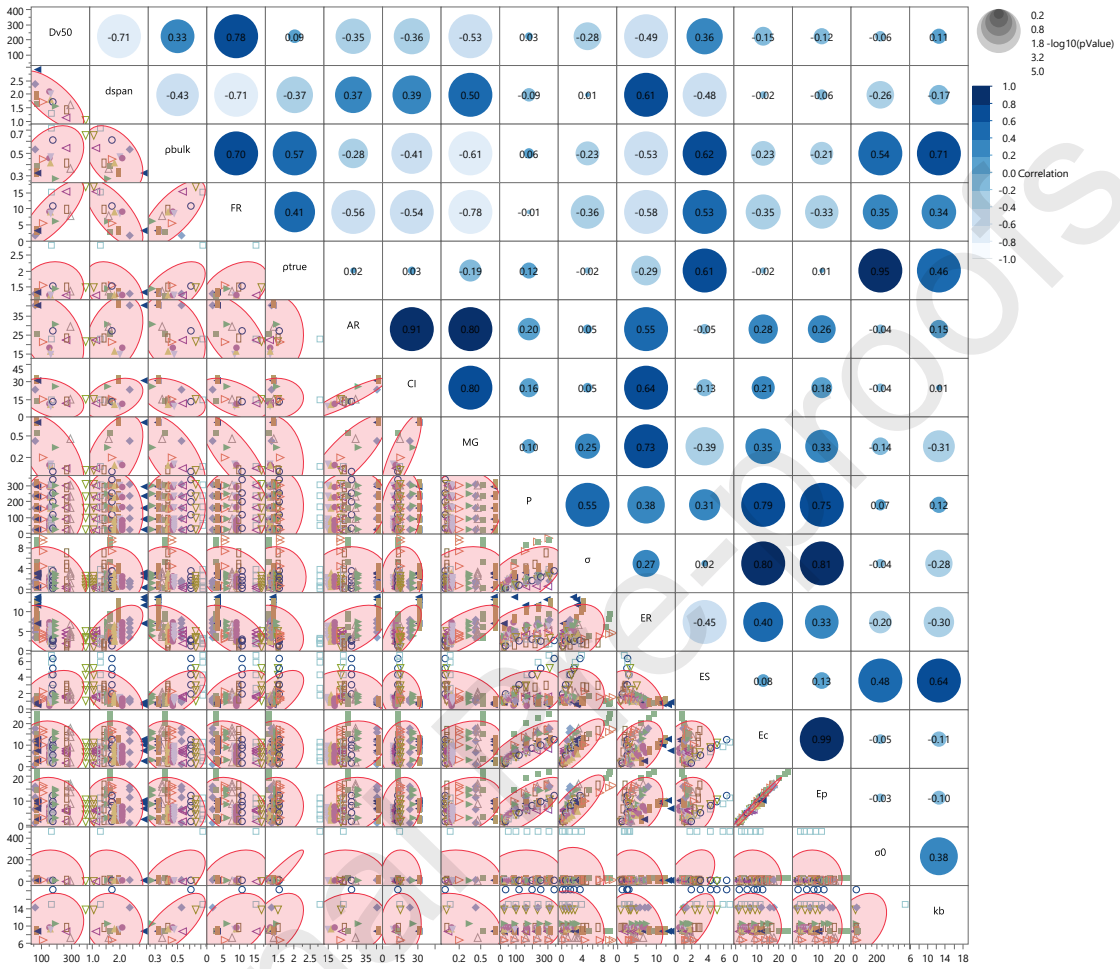

Fig. 4. Scatterplot matrix of excipient variables. The red ellipses indicate the 95% confidence density ellipses. The blue significance circles show the correlations. Each marker represents one excipient at a given compaction pressure at 80 rpm.

3.4. Principal component analysis

PCA was performed on the powder and tablet property data matrix to explore and highlight the variance within the input dataset. Typically, PCA transforms the input data into a lower dimensional set of new independent variables known as principal components (PCs). This transformation allows the capture of the highest possible variance. The loading scatter plot derived from PCA displays the spatial distribution of variables influenced by two primary PCs, which explained most variations in the data. Conversely, the score plot reveals details about the diversity among the samples, enabling discrimination of the similarities or differences between samples. When variables are highly positively correlated with each other, they are positioned in similar directions or closer to each other on the loading scatter plot. In contrast, the variables are negatively correlated when they are located on opposite sides of the plot origin. The correlation is

607 considered weaker when the descriptor is close to the origin of the loading scatter plot,
608 which is not relevant for the respective PCs. The rows on the dataset related to PEO and
609 PVA where tensile strength was not measurable were not considered for PCA. Once
610 again, to make the analysis more representative of commercial scale tableting operations,
611 a speed of 80 rpm was selected.

612 **Table 4**

613 Input variables incorporated in PCA.

PCA input variables	Symbol
Particle size	Dv10, Dv50, Dv90, dwidth and dspan
Density	ρ_{true}, ρ_{bulk}, ρ_{tapped}
Flow properties	HR, CI
Flow rate	FR
Angle of repose	AR
Compression pressure	P
Tensile strength	σ
Porosity	ε
Compressibility	Py
Compactibility	σ_0, k_b
Tabletability	b, y_{max}
Plastic energy	E_p
Compression energy	E_c
Elastic recovery	ER
Ejection stress	ES

Strain rate sensitivity	SRS
Moisture gain	MG

Fig. 6 shows the loading scatter plot (left) and the score plot (right) of the PCA of the selected data matrix composed of all studied excipients with 26 variables (Table 4). The most common method of selecting the principal components to be used is to set a threshold of cumulative explained variance. The suitability of PCA for dimension reduction can be considered when few principal components are sufficient to explain a significant part of the variance in the data. The scree plot (Fig. 5), where the percentage of the cumulative variance is explained, shows that the first four principal components explained approximately 80% of the total variation, of which the contributions of the first two components to the total variance were 33.2% and 20.2%, respectively, as displayed in Fig. 6.

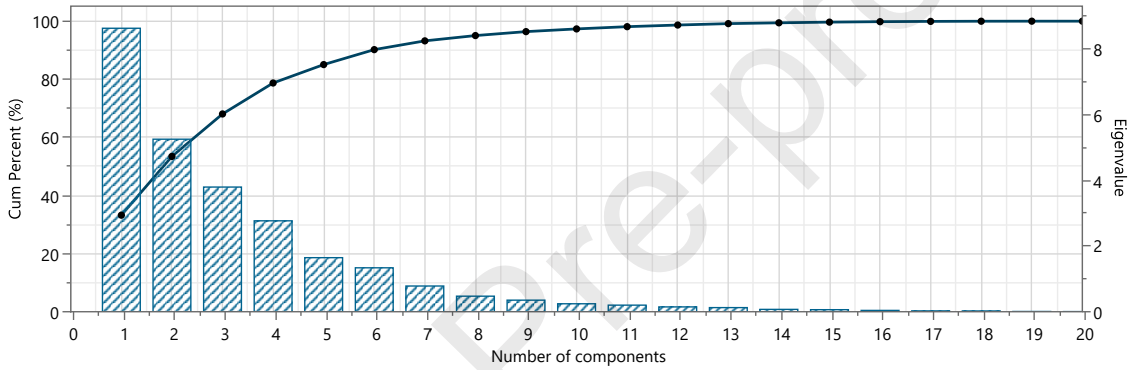

Fig. 5. PCA scree plot and percentage of the cumulative variance in the data.

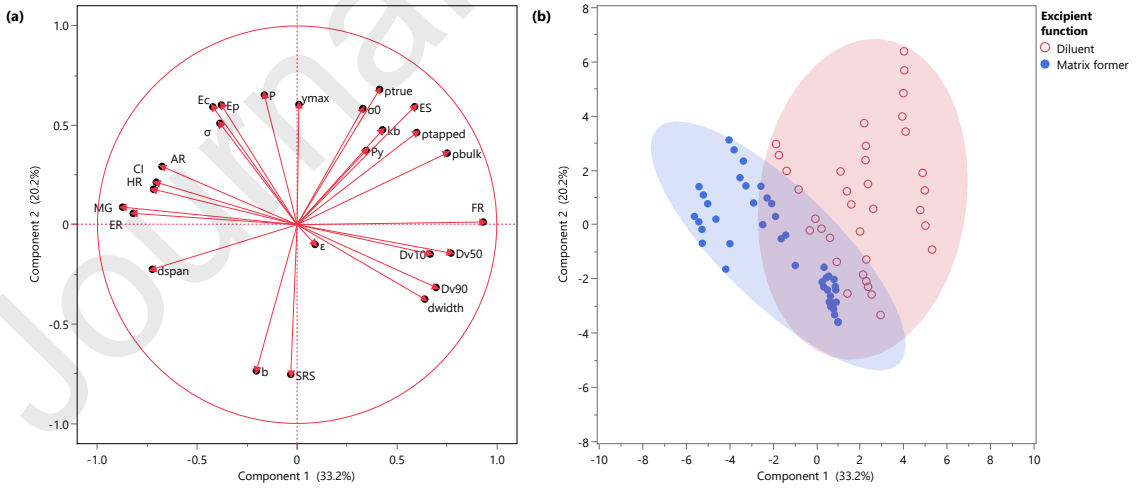

Fig. 6. PCA based on the first two components: (a) loading scatter plot and (b) score scatter plot. The colored areas indicate the 95% confidence ellipses.

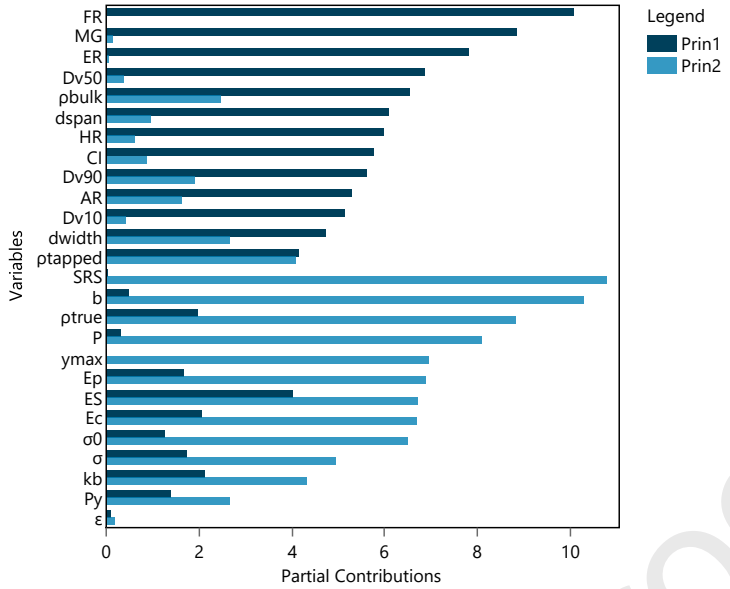

Fig. 7. Plot of partial contribution of excipient variables on PCA.

The loading scatter plot describes the contribution of each of the original variables included in the PCA (Fig. 6a). By plotting the loadings for the two PCs, it is possible to assess the relative importance of each of the variables and demonstrate how these properties influence the orientation of excipients' location on the plane. As depicted in Fig. 7, the variability of PC1 was mainly dominated by the bulk properties of powders and ER. The second PC was predominantly affected by tableting variables, with SRS, tabletability growth rate (b) and ρ_{true} showing the highest weight.

In the first principal component (PC1), it can be observed that FR is positioned to the right side of the loading scatter plot, exhibiting strong positive PC1 loading values. Conversely, HR, CI, and AR, which collectively describe the propensity of powders to be compressed, exhibit high negative PC1 loadings and are grouped together. Powders with higher CI and HR, indicating poorer flow properties and greater cohesiveness, have a higher AR and lower FR. These high negative PC1 loadings are clustered with MG and ER, suggesting that poorly flowing excipients with higher moisture content will have a relatively higher degree of expansion during the decompression phase. Moreover, moisture absorption can result in strong cohesion between particles, higher densification, and a consequent decrease in flow properties (Zhang et al., 2003). Additionally, the increase in ER may be attributable to the high moisture content due to the modification of the deformation behavior of the excipient. The ρ_{bulk} and ρ_{tapped} were also located on the positive side of PC1 and were opposite to the flow parameters (CI, HR, AR), as reported in the literature (Kim and Choi, 2022a; Wan et al., 2021). This result elucidates that materials with higher density tend to have better flow properties. Nevertheless, there are dominant forces acting on particles (gravitational, friction, adhesive and cohesive), and the mechanisms of interaction between them define flow characteristics. Moreover, the relationship between the forces and powder flow behavior is governed by a combination of several powder characteristics, such as particle size distribution, density, shape, surface properties and moisture content, and therefore should be mutually assessed (Clayton, 2019; Podczeck, 1998). In our understanding and according to the powder deformation process, there is no causal relationship between flow properties and ER. The particle size descriptors (Dv10, Dv50, Dv90 and dwidth) were grouped together in the lower right

corner (i.e., at higher PC1 and negative PC2 loadings), slightly opposite of the dspan, as illustrated by Dai et al. (2019). Particle size and flow descriptors were also negatively related. As expected, larger particles generally flow better, presenting lower values of CI and HR (Wan et al., 2021).

The loading scatter plot indicates positive PC2 loadings for ρ_{true}, σ_0, ES, y_{max}, E_p and E_c. Notably, as E_p corresponds to the total energy given to the tablet, it includes E_c, i.e., the energy given to the tablet when the force increases. Furthermore, E_p increases with increasing compression pressure because of the greater extent of particle deformation. Additionally, it is reasonably expected that the higher the energy given to the tablet during compression, the greater the σ ($R^2 = 0.802$). Although ε shows an insignificantly smaller weighting, the assessment of PC2 against PC3 (accounting for 14.9% of the overall variance) demonstrated a strong negative PC3 loading for ε (data not shown). P and ε are inversely related; as the tablet compression pressure increases, the particles become more compact, reducing the void spaces between them and decreasing the porosity (Jin et al., 2022).

The growth constant rate of the Gompertz equation (b), a reasonable predictor of material plasticity, showed high negative PC2 loadings in the opposite direction of y_{max}. Higher b values suggest a decrease in y_{max}. This y_{max} position also suggested that powders with a higher density tend to require higher pressure to form a structure exhibiting appreciable mechanical strength. This was already described by Dai et al. (2019), where tabletability was positively correlated with tensile strength and negatively correlated with density parameters. ES and Py, although partially explained by PC1 and PC2, are positively related. One possible explanation for this is associated with brittle materials that exhibit a higher degree of nonelastic deformation during loading. Strong plastic deformation reflects a higher residual radial die wall stress and, consequently, higher tablet ejection force (Takeuchi et al., 2004; Uzondu et al., 2018), which could lead to capping or lamination (Paul and Sun, 2017). Meynard et al. (2022b) developed a machine learning predictive model (decision tree classification) of capping behavior from three in-die tablet properties: the plastic energy, the in-die elastic recovery and the residual die-wall pressure. High values of plastic energy and low values of the in-die elastic recovery and residual die-wall pressure were related to formulations giving noncapped tablets. Py is also moderately anti-correlated with moisture content, possibly due to plastic materials with low yield pressure containing a significant moisture content. In HPMC, a hygroscopic material, moisture acts as a plasticizer, resulting in lower porosity and thus better compressibility (Nokhodchi et al., 1996). The compactibility of each excipient was fitted using the Ryshkewitch–Duckworth exponential equation, where the bonding capacity constant (k_b) and σ_0 were obtained. As expected, compactibility parameters are positively related to each other and positioned in the right upper corner of PCA, being moderately explained by PC2, similar to σ.

From the score scatter plot (Fig. 6b), two main clusters can be identified based on excipient function. Matrix former excipients are mostly distributed in the left half of the scatter plot, whereas the diluents are located on the right side, mainly explained by PC2. The hygroscopic nature of polymers, their ability to swell and the presence of amorphous regions can play a significant role in the diffusion of water molecules into the polymer, explaining the strong negative loading of MG on PC1. The predominant plastic deformation mechanism of polymers contributes to an increased mechanical strength under a given compression pressure, higher in-die ER and lower Py compared to diluents, as observed by the distinct positions of these variables on the loading plot. Otherwise,

while polymers act as a matrix system in formulations for extended release, the diluents chosen depend on the type of formulation and manufacturing process. Diluents used in direct compression formulations can have a variety of chemical nature and functional properties, and their intended use may differ depending on the type of formulation under development, justifying their widespread distribution along the PC2 axis. Nonetheless, diluents are positioned more on the right side, validating their high flow properties and large particle size, which provide ideal conditions for direct compression.

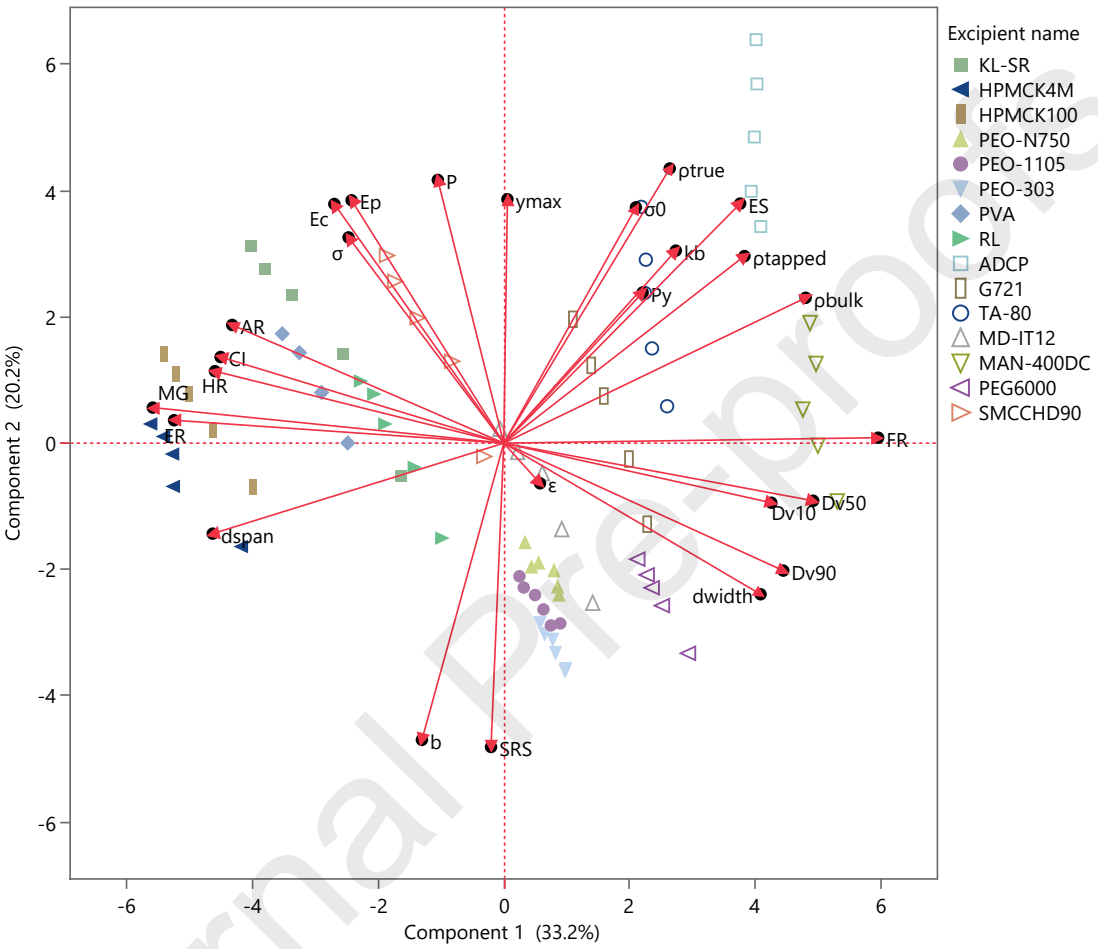

Fig. 8. PCA biplot of excipient samples and explanatory variables - PC2 against PC1.

The PCA biplot, illustrated in Fig. 8, displays the correlation scaled loading and score vectors from both variables and samples into a single plot presenting how all excipients are distributed based on how each of the variables contributes to the first two principal components. The data points are represented as colored signs whereby each excipient is displayed in one color. The loading of the input variables is represented by red lines and black points. Excipients were scattered in all quartiles of the plot, and the samples with the most similar properties were clustered together. In contrast, excipients with notably contrasting descriptors will typically be positioned at opposite sides.

Evaluating the biplot, the flow behavior can be qualitatively predicted based on the correlation between excipients and their properties. The desirable trend of flow behavior is much more dependent on PC1 than PC2. For example, excipients on the negative side of PC1 have lower ρ_{bulk} and ρ_{tapped}, higher CI and HR and higher cohesion, indicating that these powders are poorly flowing. HPMCK4M, HPMCK100 and PVA were located on

the left side of the PC1 vs PC2 score scatter plot. These materials have lower flow properties, as demonstrated by higher values of CI and HR as well as lower values of FR. Allenspach et al. (2020) investigated the flow behavior of HPMCK4M, showing high CI values and very low FR values, consistent with the obtained results. With improved flow of the direct compression HPMC grades, it would be more feasible to use these excipients in direct compression manufacturing. The highest flowability was expected for KL-SR, resulting from lower HR and CI values. The smaller particle size and higher MG most likely cause high cohesiveness, which affects flow properties (Hauschild and Picker-Freyer, 2006) and results in the KL-SR samples plotted in the upper left corner. ADCP, MAN-400DC, G721 and TA-80, with CI lower than 16%, fell on the right, based on the loading plot. These diluents with brittle-predominant deformation usually exhibit high density and excellent flow properties. These results were consistent with the literature (Bolhuis et al., 2009; Haware et al., 2009; Ilic et al., 2009). Similar patterns were observed in scatter plot PCA by Berkenkemper et al. (2023b) and Van Snick et al. (2018a), where TA-80 is positioned near density descriptors. During tablet compression, brittle materials present high Py and ES (Ilic et al., 2013; Michaut et al., 2010), which explains their same side and direction along the coordinate axis of PCs. In our analysis, the Py of brittle materials was found to be significantly higher than that of plastic materials. Overall, the order of powder yield pressure at 80 rpm is MD-IT12 (817.0 MPa) > ADCP (706.7 MPa) > TA-80 (170.9 MPa) > MAN-400DC (148.0 MPa) > G721 (102.0 MPa). The Heckel analysis reported in the literature also supports these findings, as a low slope of the linear portion of the compression curve was found for ADCP with a Py value significantly higher than that of silicified microcrystalline cellulose, confirming the plastic deformation behavior of the latter and brittle fracture of the former (Hentzschel et al., 2012). KL-SR, PEOs, and PEG6000, despite their plastic behavior, exhibited slightly more positive scores along PC1, as their flow properties are substantially better than those of other polymers. Furthermore, both PEO and PEG6000 have low melting points, which could potentially lead to an increase in ejection force during tablet compression and contribute to a higher likelihood of sticking (Meruva and Donovan, 2019). SRS was located on the far lower side of the loading scatter plot, suggesting a strong negative correlation with PC2. Speed-dependent friction (Desbois et al., 2022), viscoplasticity (David and Augsburger, 1977), viscoelasticity (Meynard et al., 2022a) or air entrapment (Casahoursat et al., 1988) are phenomena that can be involved in SRS. Low SRS is desirable, if less sensitivity to an eventual change in tableting speed on scale-up is a concern. Generally, polymeric materials known to deform plastically require more time to consolidate, making them more sensitive to speed variations (Roberts and Rowe, 1985). Therefore, the position of PEO polymers and PEG6000 on the score plot is reasonably understood. Density parameters show a negative correlation with the growth rate (b) descriptor from the Gompertz function. Powders that have a high density, such as ADCP, TA-80 and MAN-400DC (ρ_{bulk} > 0.6 g/cm^3), show an apparently linear progression of tensile strength over the pressure studied. Thoorens et al. (2015) studied the impact of microcrystalline cellulose physicochemical properties on tabletability, suggesting that ρ_{tapped} is negatively correlated with the tensile strength at 85 MPa compaction pressure. The k_b for brittle materials was higher and according to previously reported values (Jonat et al., 2005; Reynolds et al., 2017), suggesting a high capacity to create new bonds and, hence, to increase the mechanical resistance of tablets. In fact, brittle materials that experience extensive particle fragmentation during compression typically yield tablets with high tensile strength, even at significantly high porosity (e.g., 0.3-0.4). This is attributable to the increased bonding contact area (Patel et al., 2006; Reynolds et al., 2017). For the coprocessed excipient, RL, a less significant weighting

781 was found on PC1 and PC2, thus appearing in the center of the TA-80 and HPMC
782 polymers. MAN-400DC is located on the right side of the biplot and exhibits strong
783 positive PC1 loading values, certainly due to its higher particle size.

4. Conclusion

The present work provides insight into and enhances our understanding of bulk properties and tablet compression behavior of 15 different excipients commonly employed in the development and manufacturing of extended release tablets. The physical and mechanical properties of these materials were carefully characterized in terms of particle size distribution, flow properties, moisture gain, compression and sensitivity to compression speed. The relationships between tablet porosity, tensile strength and compaction pressure were used to evaluate tabletability, compactibility and compressibility. There was no significant difference in the compressibility profiles of the majority of the studied excipients. ADCP showed to be weakly compressible because it was extremely difficult to densify below a porosity of 0.3. All excipients exhibited a decrease in compact porosity with increasing compression pressure. The highest tabletability and compactibility were determined for KL-SR and SMCCHD90. Otherwise, PVA and PEG6000 demonstrated the lowest tabletability with tensile strength values below 2.0 MPa. PCA was applied to project excipient properties onto reduced dimensions and facilitate a thorough understanding of the dataset, providing valuable insights into the correlations among the variables. Two different groups of materials - diluents and polymers - could be clearly distinguished on the score plot of PCA. They differed markedly in their consolidation behavior and plasticity during the compression process. It was found that MAN-400DC, ADCP and TA-80 were suitable diluents for direct compression due to their superior flowability and tabletability. In relation to matrix formers, the results indicated that the various grades of PEO display similar and favorable flow and tableting characteristics. FR, MG, ER, and SRS were identified as having the most significant impact on the PCA loadings. The mean yield pressure, Py, obtained from the Heckel analysis, along with the Ryshkewitch-Duckworth parameters (σ_0 and k_b), were observed to exhibit a positive correlation with ES and thus provide an important information on excipient deformation behavior. By identifying the key excipient variables, it is possible to focus efforts on controlling or optimizing extended release formulation-related excipients to minimize variability. Finally, it is crucial to consider the role of the API, additional excipients, and physical interactions between them in the tablet formulation workflow. The results also suggest further employing QbD tools, such as risk assessment or DoE, to assess how formulation variables (e.g., polymer amount, compression pressure) affect drug product compaction behavior. In summary, this study offers additional insights into how the physical properties of various excipients influence the quality attributes of tablets. Because commercial scale tableting operations can be hampered by poorly characterized raw material properties, this work is considered a useful tool for limiting resource consumption in early drug product development, ultimately saving time and resources.

CRediT authorship contribution statement

Ana Sofia Sousa: Conceptualization, methodology, investigation, writing – original draft, Visualization. **João Serra:** Conceptualization, supervision. **Catarina Estevens:** Writing – review & editing. **Ricardo Costa:** Conceptualization, Writing – review & editing. **António José Ribeiro:** Conceptualization, writing – review & editing, supervision.

Declaration of Competing Interest

The authors declare that they have no known competing financial interests or personal relationships that could have appeared to influence the work reported in this paper.

Acknowledgments

Ana Sofia Sousa acknowledges the PhD grant PD/BDE/150736/2020, assigned by FCT (Fundação para a Ciência e Tecnologia, Portugal) and the Tecnimede Group from Drugs R&D Doctoral Program.

Appendix A. Supplementary material

Supplementary data for this article can be found online at

Data availability

Data will be made available on request.

References

Al-Nasassrah, M.A., Podczeck, F., Newton, J.M., 1998. The effect of an increase in chain length on the mechanical properties of polyethylene glycols. Eur. J. Pharm. Biopharm. 46, 31-38. https://doi.org/10.1016/s0939-6411(97)00151-3.

Alderborn, G., Nystrom, C., 1996. Pharmaceutical powder compaction technology. Marcel Dekker, Inc., New York.

Allenspach, C., Timmins, P., Sharif, S., Minko, T., 2020. Characterization of a novel hydroxypropyl methylcellulose (HPMC) direct compression grade excipient for pharmaceutical tablets. Int. J. Pharm. 583, 119343. https://doi.org/10.1016/j.ijpharm.2020.119343.

Armstrong, N.A., Hainesnu.Rf, 1974. Elastic recovery and surface-area changes in compacted powder systems. Powder Technol. 9, 287-290. https://doi.org/10.1016/0032-5910(74)80054-9.

Bekaert, B., Penne, L., Grymonpre, W., Van Snick, B., Dhondt, J., Boeckx, J., Vogeleer, J., De Beer, T., Vervaet, C., Vanhoorne, V., 2021. Determination of a quantitative relationship between material properties, process settings and screw feeding behavior via multivariate data-analysis. Int. J. Pharm. 602, 120603. https://doi.org/10.1016/j.ijpharm.2021.120603.

Benedetti, A., Khoo, J., Sharma, S., Facco, P., Barolo, M., Zomer, S., 2019. Data analytics on raw material properties to accelerate pharmaceutical drug development. Int. J. Pharm. 563, 122-134. https://doi.org/10.1016/j.ijpharm.2019.04.002.

Berkenkemper, S., Kleinebudde, P., 2022. Compressibility analysis as robust in-die compression analysis for describing tableting behaviour. RPS Pharmacy and Pharmacology Reports 1, 1-7. https://doi.org/10.1093/rpsppr/rqac004.

Berkenkemper, S., Klinken, S., Kleinebudde, P., 2023a. Investigating compressibility descriptors for binary mixtures of different deformation behavior. Powder Technol., 118571. https://doi.org/10.1016/j.powtec.2023.118571.

Berkenkemper, S., Klinken, S., Kleinebudde, P., 2023b. Multivariate data analysis to evaluate commonly used compression descriptors. Int. J. Pharm. 637, 122890. https://doi.org/10.1016/j.ijpharm.2023.122890.

Bolhuis, G.K., Engelhart, J.J.P., Eissens, A.C., 2009. Compaction properties of isomalt. Eur. J. Pharm. Biopharm. 72, 621-625. https://doi.org/10.1016/j.ejpb.2009.03.005.

Bourduche, F., Sanchez-Ballester, N.M., Bataille, B., Lefevre, P., Sharkawi, T., 2020. Structure-Property Relationship of Amorphous Maltitol as Tableting Excipient. AAPS PharmSciTech 21, 281. https://doi.org/10.1208/s12249-020-01824-8.

Caccavo, D., Lamberti, G., Barba, A.A., Abrahmsen-Alami, S., Viriden, A., Larsson, A., 2017. Effects of HPMC substituent pattern on water up-take, polymer and drug release: An experimental and modelling study. Int. J. Pharm. 528, 705-713. https://doi.org/10.1016/j.ijpharm.2017.06.064.

Carlin, B., 2008. Direct Compression and the Role of Filler-binders, in: Augsburger, L.L., Hoag, S.W. (Eds.), Pharmaceutical Dosage Forms: Tablets. Taylor & Francis Group, Boca Raton, pp. 173-216.

Carlin, B., 2018. The Role of Excipients in Quality by Design (QbD), in: Schlindwein, W., Gibson, M. (Eds.), Pharmaceutical Quality by Design: A Practical Approach. John Wiley & Sons Ltd., New Jersey, pp. 97-116.

879 Casahoursat, L., Lemagnen, G., Larrouture, D., 1988. The use of stress relaxation trials to
880 characterize tablet capping. Drug Dev. Ind. Pharm. 14, 2179-2199.
881 https://doi.org/10.3109/03639048809152010.

882 Cirin-Varadan, S., Duris, J., Mirkovic, M., Ivanovic, M., Parojcic, J., Aleksic, I., 2022.
883 Comparative evaluation of mechanical properties of lactose-based excipients co-processed with
884 lipophilic glycerides as meltable binders. J. Drug Deliv. Sci. Technol. 67, 102981.
885 https://doi.org/10.1016/j.jddst.2021.102981.

886 Clayton, J., 2019. An Introduction to Powder Characterization, in: Narang, A.S., Badawy, S.I.F.
887 (Eds.), Handbook of Pharmaceutical Wet Granulation: Theory and Practice in a Quality by Design
888 Paradigm. Acadmic Press, Cambridge, MA, USA, pp. 569-613.

889 Colombo, P., Santi, P., Siepmann, J., Colombo, G., Sonvico, F., Rossi, A., Strusi, L., 2008.
890 Swellable and rigid matrices: Controlled release matrices with cellulose ethers, in: Augsburger,
891 L.L., Hoag, S.W. (Eds.), Pharmaceutical Dosage Forms: Tablets. Taylor & Francis Group, Boca
892 Raton, pp. 433-468.

893 Dai, S.Y., Xu, B., Zhang, Z.Q., Yu, J.Q., Wang, F., Shi, X.Y., Qiao, Y.J., 2019. A compression
894 behavior classification system of pharmaceutical powders for accelerating direct compression
895 tablet formulation design. Int. J. Pharm. 572, 118742.
896 https://doi.org/10.1016/j.ijpharm.2019.118742.

897 Dave, V.S., Saoji, S.D., Raut, N.A., Haware, R.V., 2015. Excipient Variability and Its Impact on
898 Dosage Form Functionality. J. Pharm. Sci. 104, 906-915. https://doi.org/10.1002/jps.24299.

899 David, S.T., Augsburger, L.L., 1977. Plastic flow during compression of directly compressible
900 fillers and its effect on tablet strength. J. Pharm. Sci. 66, 155-159.
901 https://doi.org/10.1002/jps.2600660205.

902 de Backere, C., De Beer, T., Vervaet, C., Vanhoorne, V., 2022. Effect of feed frame on lubricant
903 sensitivity during upscaling from a compaction simulator to a rotary tablet press. Int. J. Pharm.
904 616, 121562. https://doi.org/10.1016/j.ijpharm.2022.121562.

905 Desbois, L., Tchoreloff, P., Mazel, V., 2022. Use of jump-tests for the characterization of the
906 viscoplastic behavior of pharmaceutical powders during compaction. Powder Technol. 404,
907 117406. https://doi.org/10.1016/j.powtec.2022.117406.

908 Dhondt, J., Bertels, J., Kumar, A., Van Hauwermeiren, D., Ryckaert, A., Van Snick, B.,
909 Klingeleers, D., Vervaet, C., De Beer, T., 2022. A multivariate formulation and process
910 development platform for direct compression. Int. J. Pharm. 623, 121962.
911 https://doi.org/10.1016/j.ijpharm.2022.121962.

912 Duckworth, W., 1953. Discussion of Ryshkewitch Paper. J. Am. Ceram. Soc. 36, 68.

913 Escotet-Espinoza, M.S., Moghtadernejad, S., Scicolone, J., Wang, Y.F., Pereira, G., Schafer, E.,
914 Vigh, T., Klingeleers, D., Ierapetritou, M., Muzzio, F.J., 2018. Using a material property library
915 to find surrogate materials for pharmaceutical process development. Powder Technol. 339, 659-
916 676. https://doi.org/10.1016/j.powtec.2018.08.042.

917 Fell, J., Newton, J., 1970. Determination of tablet strength by the diametral-compression test. J.
918 Pharm. Sci. 59, 688-691. https://doi.org/10.1002/jps.2600590523.

919 Garekani, H.A., Ford, J.L., Rubinstein, M.H., Rajabi-Siahboomi, A.R., 2001. Effect of
920 compression force, compression speed, and particle size on the compression properties of
921 paracetamol. Drug Dev. Ind. Pharm. 27, 935-942. https://doi.org/10.1081/ddc-100107674.

Ghori, M.U., 2016. Powder Compaction: Compression Properties of Cellulose Ethers. Br. J. Pharm. 1, 19-29. https://doi.org/10.5920/bjpharm.2016.09.

Grdesic, P., Paudel, A., Ilic, I.G., 2020. High-Molecular-Weight Hypromellose from Three Different Suppliers: Effects of Compression Speed, Tableting Equipment, and Moisture on the Compaction. AAPS PharmSciTech 21, 203. https://doi.org/10.1208/s12249-020-01688-y.

Grymonpre, W., Vanhoorne, V., Van Snick, B., Prudilova, B.B., Detobel, F., Remon, J.P., De Beer, T., Vervaet, C., 2018. Optimizing feed frame design and tableting process parameters to increase die-filling uniformity on a high-speed rotary tablet press. Int. J. Pharm. 548, 54-61. https://doi.org/10.1016/j.ijpharm.2018.06.047.

Hauschild, K., Picker-Freyer, K.M., 2006. Evaluation of tableting and tablet properties of Kollidon SR: The influence of moisture and mixtures with theophylline monohydrate. Pharm. Dev. Technol. 11, 125-140. https://doi.org/10.1080/10837450500464289.

Haware, R.V., Bauer-Brandl, A., Tho, I., 2010. Comparative evaluation of the powder and compression properties of various grades and brands of microcrystalline cellulose by multivariate methods. Pharm. Dev. Technol. 15, 394-404. https://doi.org/10.3109/10837450903262041.

Haware, R.V., Tho, I., Bauer-Brandl, A., 2009. Multivariate analysis of relationships between material properties, process parameters and tablet tensile strength for alpha-lactose monohydrates. Eur. J. Pharm. Biopharm. 73, 424-431. https://doi.org/10.1016/j.ejpb.2009.08.005.

Hayashi, Y., Nakano, Y., Marumo, Y., Kumada, S., Okada, K., Onuki, Y., 2021. Application of machine learning to a material library for modeling of relationships between material properties and tablet properties. Int. J. Pharm. 609, 121158. https://doi.org/10.1016/j.ijpharm.2021.121158.

Heckel, R.W., 1961. Density-Pressure Relationships in Powder Compaction. Trans. Am. Inst. 221, 671-675.

Hentzschel, C.M., Sakmann, A., Leopold, C.S., 2012. Comparison of traditional and novel tableting excipients: Physical and compaction properties. Pharm. Dev. Technol. 17, 649-653. https://doi.org/10.3109/10837450.2011.572897.

Ilic, I., Govedarica, B., Sibanc, R., Dreu, R., Srcic, S., 2013. Deformation properties of pharmaceutical excipients determined using an in-die and out-die method. Int. J. Pharm. 446, 6-15. https://doi.org/10.1016/j.ijpharm.2013.02.001.

Ilic, I., Kasa, P., Dreu, R., Pintye-Hodi, K., Srcic, S., 2009. The compressibility and compactibility of different types of lactose. Drug Dev. Ind. Pharm. 35, 1271-1280. https://doi.org/10.1080/03639040902932945.

Ilyes, K., Casian, T., Hales, D., Borodi, G., Rus, L., Stiufiuc, R., Tomuta, I., 2021. Applying the principles of Quality by Design (QbD) coupled with Multivariate Data Analysis (MVDA) in establishing the impact of raw material variability for extended release tablets. Farmacia 69, 481-497. https://doi.org/10.31925/farmacia.2021.3.11.

Jin, C., Zhao, L.J., Feng, Y., Hong, Y.L., Shen, L., Lin, X., 2022. Simultaneous modeling prediction of three key quality attributes of tablets by powder physical properties. Int. J. Pharm. 628, 122344. https://doi.org/10.1016/j.ijpharm.2022.122344.

Jonat, S., Hasenzahl, S., Gray, A., Schmidt, P.C., 2005. Influence of compacted hydrophobic and hydrophilic colloidal silicon dioxide on tableting properties of pharmaceutical excipients. Drug Dev. Ind. Pharm. 31, 687-696. https://doi.org/10.1080/03639040500216451.

964 Kim, J.Y., Choi, D., 2022a. Control Strategy for Excipient Variability in the Quality by Design
965 Approach Using Statistical Analysis and Predictive Model: Effect of Microcrystalline Cellulose
966 Variability on Design Space. Pharmaceutics 14, 2416.
967 https://doi.org/10.3390/pharmaceutics14112416.

968 Kim, J.Y., Choi, D., 2022b. Quality by design approach with multivariate analysis and artificial
969 neural network models to understand and control excipient variability. J. Pharm. Investig.
970 https://doi.org/10.1007/s40005-022-00608-5.

971 Kosir, D., Ojstersek, T., Baumgartner, S., Vrecer, F., 2018. A study of critical functionality-
972 related characteristics of HPMC for sustained-release tablets. Pharm. Dev. Technol. 23, 865-873.
973 https://doi.org/10.1080/10837450.2016.1264417.

974 Larhrib, H., Wells, J.I., 1998. Compression speed on polyethylene glycol and dicalcium
975 phosphate tableted mixtures. Int. J. Pharm. 160, 197-206. https://doi.org/10.1016/s0378-
976 5173(97)00309-8.

977 Leane, M., Pitt, K., Reynolds, G., Mfg Classification Syst, M.C.S.W., 2015. A proposal for a drug
978 product Manufacturing Classification System (MCS) for oral solid dosage forms. Pharm. Dev.
979 Technol. 20, 12-21. https://doi.org/10.3109/10837450.2014.954728.

980 Lieberman, H.A., Lachman, L.S., J.B., 1989. Pharmaceutical dosage forms: tablets. Marcel
981 Dekker Inc., New York.

982 Maderuelo, C., Zarzuelo, A., Lanao, J.M., 2011. Critical factors in the release of drugs from
983 sustained release hydrophilic matrices. J. Control Release 154, 2-19.
984 https://doi.org/10.1016/j.jconrel.2011.04.002.

985 Meruva, S., Donovan, M.D., 2019. Polyethylene Oxide (PEO) Molecular Weight Effects on
986 Abuse-Deterrent Properties of Matrix Tablets. AAPS PharmSciTech 21, 28.
987 https://doi.org/10.1208/s12249-019-1565-y.

988 Meynard, J., Amado-Becker, F., Tchoreloff, P., Mazel, V., 2022a. Characterization of the
989 viscoelasticity of pharmaceutical tablets using impulse excitation technique. Int. J. Pharm. 613,
990 121410. https://doi.org/10.1016/j.ijpharm.2021.121410.

991 Meynard, J., Amado-Becker, F., Tchoreloff, P., Mazel, V., 2022b. On the complexity of
992 predicting tablet capping. Int. J. Pharm. 623, 121949.
993 https://doi.org/https://doi.org/10.1016/j.ijpharm.2022.121949.

994 Michaut, F., Busignies, V., Fouquereau, C., De Barochez, B.H., Leclerc, B., Tchoreloff, P., 2010.
995 Evaluation of a Rotary Tablet Press Simulator as a Tool for the Characterization of Compaction
996 Properties of Pharmaceutical Products. J. Pharm. Sci. 99, 2874-2885.
997 https://doi.org/10.1002/jps.22032.

998 Moreton, C., 2010. Functionality and Performance of Excipients in a Quality-by-Design World.
999 Am. Pharm. Rev. 12.

1000 Muzikova, J., Komersova, A., Lochar, V., Vildova, L., Vosoustova, B., Bartos, M., 2018.
1001 Comparative evaluation of the use of dry binders in a physical mixture or as a coprocessed dry
1002 binder in matrix tablets with extended drug release. Acta Pharm. 68, 295-311.
1003 https://doi.org/10.2478/acph-2018-0030.

1004 Nokhodchi, A., Ford, J.L., Rowe, P.H., Rubinstein, M.H., 1996. The effect of moisture on the
1005 Heckel and energy analysis of hydroxypropylmethylcellulose 2208 (HPMC K4M). Journal of

Pharmacy and Pharmacology 48, 1122-1127. https://doi.org/10.1111/j.2042-7158.1996.tb03906.x.

Osamura, T., Takeuchi, Y., Onodera, R., Kitamura, M., Takahashi, Y., Tahara, K., Takeuchi, H., 2016. Characterization of tableting properties measured with a multi-functional compaction instrument for several pharmaceutical excipients and actual tablet formulations. Int. J. Pharm. 510, 195-202. https://doi.org/10.1016/j.ijpharm.2016.05.024.

Patel, S., Kaushal, A.M., Bansal, A.K., 2006. Compression physics in the formulation development of tablets. Critical Reviews in Therapeutic Drug Carrier Systems 23, 1-65.

Paul, S., Sun, C.C., 2017. Gaining insight into tablet capping tendency from compaction simulation. Int. J. Pharm. 524, 111-120. https://doi.org/10.1016/j.ijpharm.2017.03.073.

Picker, K.M., 2001. Time dependence of elastic recovery for characterization of tableting materials. Pharm. Dev. Technol. 6, 61-70. https://doi.org/10.1081/pdt-100000014.

Pitt, K.G., Heasley, M.G., 2013. Determination of the tensile strength of elongated tablets. Powder Technol. 238, 169-175. https://doi.org/10.1016/j.powtec.2011.12.060.

Podczeck, F., 1998. Particle-particle adhesion in pharmaceutical powder handling. Imperial College Press, London.

Podczeck, F., 2012. Methods for the practical determination of the mechanical strength of tablets-From empiricism to science. Int. J. Pharm. 436, 214-232. https://doi.org/10.1016/j.ijpharm.2012.06.059.

Portier, C., Vigh, T., Di Pretoro, G., Leys, J., Klingeleers, D., De Beer, T., Vervaet, C., Vanhoorne, V., 2021. Continuous twin screw granulation: Impact of microcrystalline cellulose batch-to-batch variability during granulation and drying - A QbD approach. Int. J. Pharm.: X. 3, 100077. https://doi.org/10.1016/j.ijpx.2021.100077.

Reynolds, G.K., Campbell, J.I., Roberts, R.J., 2017. A compressibility based model for predicting the tensile strength of directly compressed pharmaceutical powder mixtures. Int. J. Pharm. 531, 215-224. https://doi.org/10.1016/j.ijpharm.2017.08.075.

Roberts, R.J., Rowe, R.C., 1985. The effect of punch velocity on the compaction of a variety of materials. Journal of Pharmacy and Pharmacology 37, 377-384. https://doi.org/10.1111/j.2042-7158.1985.tb03019.x.

Roopwani, R., Buckner, I.S., 2021. Understanding Deformation Behavior and Compression Speed Effect in Gabapentin Compacts. J. Pharm. Sci. 110, 2157-2166. https://doi.org/10.1016/j.xphs.2020.12.021.

Rue, P.J., Rees, J.E., 1978. Limitations of the Heckel relation for predicting powder compaction mechanisms. J Pharm Pharmacol 30, 642-643. https://doi.org/10.1111/j.2042-7158.1978.tb13347.x.

Sonnergaard, J.M., 1999. A critical evaluation of the Heckel equation. Int. J. Pharm. 193, 63-71. https://doi.org/10.1016/s0378-5173(99)00319-1.

Sousa, A.S., Serra, J., Estevens, C., Costa, R., Ribeiro, A.J., 2022. A quality by design approach in oral extended release drug delivery systems: where we are and where we are going? J. Pharm. Investig. https://doi.org/10.1007/s40005-022-00603-w.

Sun, C.C., 2016. A classification system for tableting behaviors of binary powder mixtures. Asian J. Pharm. Sci. 11, 486-491. https://doi.org/10.1016/j.ajps.2015.11.122.

Takeuchi, H., Nagira, S., Yamamoto, H., Kawashima, Y., 2004. Die wall pressure measurement for evaluation of compaction property of pharmaceutical materials. Int. J. Pharm. 274, 131-138. https://doi.org/10.1016/j.ijpharm.2004.01.008.

Thakkar, S., Sharma, K., Khurana, S., Bansal, A.K., 2016. Excipients and their functionality for enabling technologies in oral dosage forms, in: Koo, O.M.Y. (Ed.), Pharmaceutical Excipients: Properties, Functionality, and Applications in Research and Industry. John Wiley & Sons, Inc., New Jersey, pp. 97-143.

Thoorens, G., Krier, F., Rozet, E., Carlin, B., Evrard, B., 2015. Understanding the impact of microcrystalline cellulose physicochemical properties on tabletability. Int. J. Pharm. 490, 47-54. https://doi.org/10.1016/j.ijpharm.2015.05.026.

Timmins, P., Pygall, S., Melia, C.D., 2014. Hydrophilic Matrix Tablets for Oral Controlled Release. Springer-Verlag, New York.

Tobyn, M., Ferreira, A.P., Lightfoot, J., Martin, E.B., Ghimire, M., Vesey, C., Kasuboski-Freeman, A., Rajabi-Siahboomi, A., 2018. Multivariate analysis as a method to understand variability in a complex excipient, and its contribution to formulation performance. Pharm. Dev. Technol. 23, 1146-1155. https://doi.org/10.1080/10837450.2018.1534862.

USP 40-NF 35, 2017. Chapter <1062> Tablet Compression Characterization. The United States Pharmacopeia and National Formulary. US Pharmacopeial Convention, Rockville.

Uzondu, B., Leung, L.Y., Mao, C., Yang, C.Y., 2018. A mechanistic study on tablet ejection force and its sensitivity to lubrication for pharmaceutical powders. Int. J. Pharm. 543, 234-244. https://doi.org/10.1016/j.ijpharm.2018.03.064.

Van Snick, B., Dhondt, J., Pandelaere, K., Bertels, J., Mertens, R., Klingeleers, D., Di Pretoro, G., Remon, J.P., Vervaet, C., De Beer, T., Vanhoorne, V., 2018a. A multivariate raw material property database to facilitate drug product development and enable in-silico design of pharmaceutical dry powder processes. Int. J. Pharm. 549, 415-435. https://doi.org/10.1016/j.ijpharm.2018.08.014.

Van Snick, B., Grymonpre, W., Dhondt, J., Pandelaere, K., Di Pretoro, G., Remon, J.P., De Beer, T., Vervaet, C., Vanhoorne, V., 2018b. Impact of blend properties on die filling during tableting. Int. J. Pharm. 549, 476-488. https://doi.org/10.1016/j.ijpharm.2018.08.015.

Van Snick, B., Kumar, A., Verstraeten, M., Pandelaere, K., Dhondt, J., Di Pretoro, G., De Beer, T., Vervaet, C., Vanhoorne, V., 2019. Impact of material properties and process variables on the residence time distribution in twin screw feeding equipment. Int. J. Pharm. 556, 200-216. https://doi.org/10.1016/j.ijpharm.2018.11.076.

Vanhoorne, V., Vervaet, C., 2020. Recent progress in continuous manufacturing of oral solid dosage forms. Int. J. Pharm. 579, 119194. https://doi.org/10.1016/j.ijpharm.2020.119194.

Vanza, J.D., Patel, R.B., Dave, R.R., Patel, M.R., 2020. Polyethylene oxide and its controlled release properties in hydrophilic matrix tablets for oral administration. Pharm. Dev. Technol. 25, 1169-1187. https://doi.org/10.1080/10837450.2020.1808015.

Vreeman, G., Sun, C.C., 2021. Mean yield pressure from the in-die Heckel analysis is a reliable plasticity parameter. Int. J. Pharm.: X. 3, 100094. https://doi.org/10.1016/j.ijpx.2021.100094.

1088 Vreeman, G., Sun, C.C., 2022a. Air entrapment during tablet compression - Diagnosis, impact on
1089 tableting performance, and mitigation strategies. Int. J. Pharm. 615, 121514.
1090 https://doi.org/10.1016/j.ijpharm.2022.121514.

1091 Vreeman, G., Sun, C.C., 2022b. A powder tabletability equation. Powder Technol. 408, 117709.
1092 https://doi.org/10.1016/j.powtec.2022.117709.

1093 Wan, S.L., Dai, C.Y., Bai, Y.L., Xie, W.Y., Guan, T.B., Sun, H.M., Wang, B.C., 2021.
1094 Application of Multivariate Methods to Evaluate Differential Material Attributes of HPMC from
1095 Different Sources. ACS Omega 6, 28598-28610. https://doi.org/10.1021/acsomega.1c03009.

1096 Wang, T., Ibrahim, A., Hoag, S.W., 2020. Understanding the impact of magnesium stearate
1097 variability on tableting performance using a multivariate modeling approach. Pharm. Dev.
1098 Technol. 25, 76-88. https://doi.org/10.1080/10837450.2019.1673774.

1099 White, L.R., Molloy, M., Shaw, R.J., Reynolds, G.K., 2022. System model driven selection of
1100 robust tablet manufacturing processes based on drug loading and formulation physical attributes.
1101 Eur. J. Pharm. Sci. 172, 106140. https://doi.org/10.1016/j.ejps.2022.106140.

1102 Worku, Z.A., Kumar, D., Gomes, J.V., He, Y.L., Glennon, B., Ramisetty, K.A., Rasmuson, A.C.,
1103 O'Connell, P., Gallagher, K.H., Woods, T., Shastri, N.R., Healy, A.M., 2017. Modelling and
1104 understanding powder flow properties and compactability of selected active pharmaceutical
1105 ingredients, excipients and physical mixtures from critical material properties. Int. J. Pharm. 531,
1106 191-204. https://doi.org/10.1016/j.ijpharm.2017.08.063.

1107 Yang, L.B., Venkatesh, G., Fassihi, R., 1996. Characterization of compressibility and
1108 compactibility of poly(ethylene oxide) polymers for modified release application by compaction
1109 simulator. J. Pharm. Sci. 85, 1085-1090. https://doi.org/10.1021/js960039v.

1110 Yost, E., Mazel, V., Sluga, K.K., Nagapudi, K., Muliadi, A.R., 2022. Beyond Brittle/Ductile
1111 Classification: Applying Proper Constitutive Mechanical Metrics to Understand the Compression
1112 Characteristics of Pharmaceutical Materials. J. Pharm. Sci. 111, 1984-1991.
1113 https://doi.org/10.1016/j.xphs.2022.01.004.

1114 Yu, D.Y., Seelam, R.R., Zhang, F., Byrn, S.R., Hoag, S.W., 2021a. Evaluation of tableting
1115 performance of Poly (ethylene oxide) in abuse-deterrent formulations using compaction
1116 simulation studies. J. Pharm. Sci. 110, 2789-2799. https://doi.org/10.1016/j.xphs.2021.03.008.

1117 Yu, Y.T., Zhao, L.J., Lin, X., Wang, Y.J., Du, R.F., Feng, Y., 2021b. Research on the powder
1118 classification and the key parameters affecting tablet qualities for direct compaction based on
1119 powder functional properties. Adv. Powder Technol. 32, 565-581.
1120 https://doi.org/10.1016/j.apt.2021.01.002.

1121 Zarmpi, P., Flanagan, T., Meehan, E., Mann, J., Fotaki, N., 2020. Impact of Magnesium Stearate
1122 Presence and Variability on Drug Apparent Solubility Based on Drug Physicochemical
1123 Properties. AAPS J. 22, 75. https://doi.org/10.1208/s12248-020-00449-w.

1124 Zhang, Y., Law, Y., Chakrabarti, S., 2003. Physical properties and compact analysis of commonly
1125 used direct compression binders. AAPS PharmSciTech 4, 489-499.
1126 https://doi.org/10.1208/pt040462.

1127 Zhang, Y., Xu, B., Wang, X., Dai, S.Y., Shi, X.Y., Qiao, Y.J., 2019. Optimal Selection of
1128 Incoming Materials from the Inventory for Achieving the Target Drug Release Profile of High
1129 Drug Load Sustained-Release Matrix Tablet. AAPS PharmSciTech 20, 76.
1130 https://doi.org/10.1208/s12249-018-1268-9.

Zhang, Y., Xu, B., Wang, X., Dai, S.Y., Sun, F., Ma, Q., Shi, X.Y., Qiao, Y.J., 2018. Setting up multivariate specifications on critical raw material attributes to ensure consistent drug dissolution from high drug-load sustained-release matrix tablet. Drug Dev. Ind. Pharm. 44, 1733-1743. https://doi.org/10.1080/03639045.2018.1492608.

Zhao, H.Y., Zhao, L.J., Lin, X., Shen, L., 2022. An update on microcrystalline cellulose in direct compression: Functionality, critical material attributes, and co-processed excipients. Carbohydr. Polym. 278, 118968. https://doi.org/10.1016/j.carbpol.2021.118968.

Zhou, D.L., Law, D., Reynolds, J., Davis, L., Smith, C., Torres, J.L., Dave, V., Gopinathan, N., Hernandez, D.T., Springman, M.K., Zhou, C.C., 2014. Understanding and Managing the Impact of HPMC Variability on Drug Release from Controlled Release Formulations. J. Pharm. Sci. 103, 1664-1672. https://doi.org/10.1002/jps.23953.

CRediT authorship contribution statement

Ana Sofia Sousa: Conceptualization, Methodology, Investigation, Writing – original draft, Visualization.

João Serra: Conceptualization, Supervision.

Catarina Estevens: Writing – review & editing.

Ricardo Costa: Conceptualization, Writing – review & editing.

António José Ribeiro: Conceptualization, Writing – review & editing, Supervision.

Declaration of interests

☒ The authors declare that they have no known competing financial interests or personal relationships that could have appeared to influence the work reported in this paper.

☐ The authors declare the following financial interests/personal relationships which may be considered as potential competing interests:

Figure captions

1167 Fig. 9. USP <1062> tablet compression characterization based on the relationships
1168 between tensile strength, solid fraction, and compaction pressure.

1169 Fig. 10. Particle size analysis of the excipients: percentile values of Dv10, Dv50 and Dv90
1170 (a), dspan (b) and particle size distribution (c).

1171 Fig. 11. Compressibility (a), tabletability (b) and compactibility (c) profiles of the
1172 investigated excipients at 80 rpm. The solid lines and markers represent the polymers and
1173 the open markers and dashed lines represent the diluents.

1174 Fig. 12. Scatterplot matrix of excipient variables. The red ellipses indicate the 95%
1175 confidence density ellipses. The blue significance circles show the correlations. Each
1176 marker represents one excipient at a given compaction pressure at 80 rpm.

1177 Fig. 13. PCA scree plot and percentage of the cumulative variance in the data.

1178 Fig. 14. PCA based on the first two components: (a) loading scatter plot and (b) score
1179 scatter plot. The colored areas indicate the 95% confidence ellipses.

1180 Fig. 15. Plot of partial contribution of excipient variables on PCA.

1181 Fig. 16. PCA biplot of excipient samples and explanatory variables - PC2 against PC1.

1182

1183

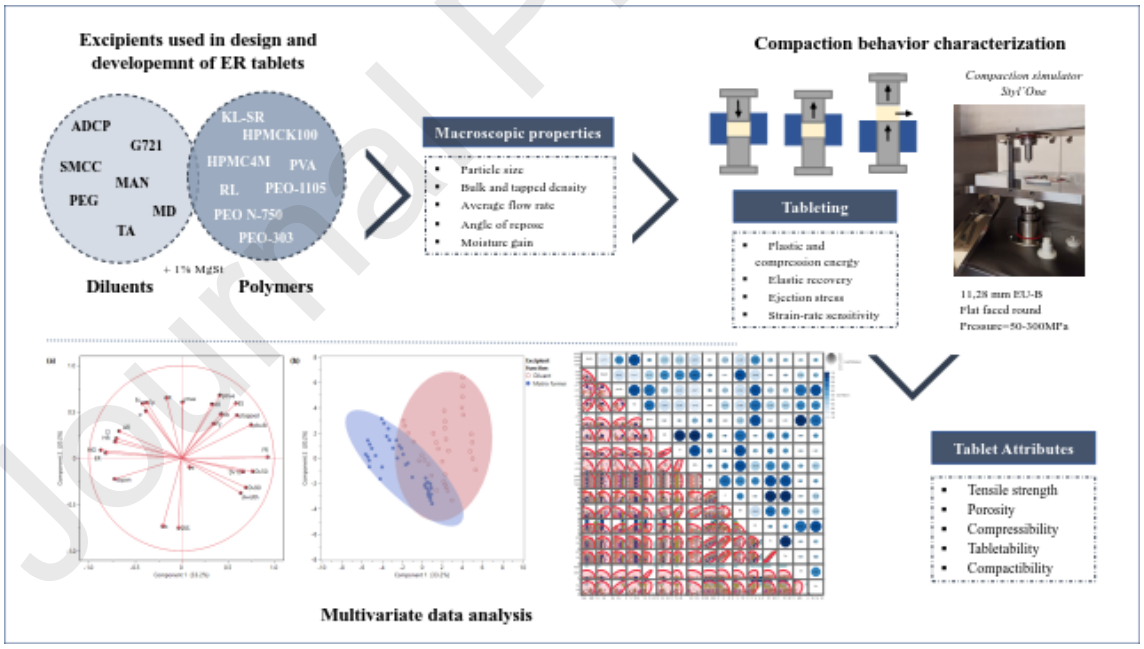

1184